ANALYSIS OF DIGITIZATION ACCURACY AND TYPICAL MISTAKES IN OLD COMPILATION

S.Dunaeva

Consultant of IAEA Nuclear Data Section

THE MAIN PROBLEMS:

1. *non-linear scales (usual problem of old publications)*
2. *scanner resolution (microscope, 'graphpen' or ruler were used before modern scanner)*
3. *angle not equal 90. degr.*

Non-linear scales? – for linear scale distance between scale marks should be equal in scanner (or screen) units when they are equal in figure units.

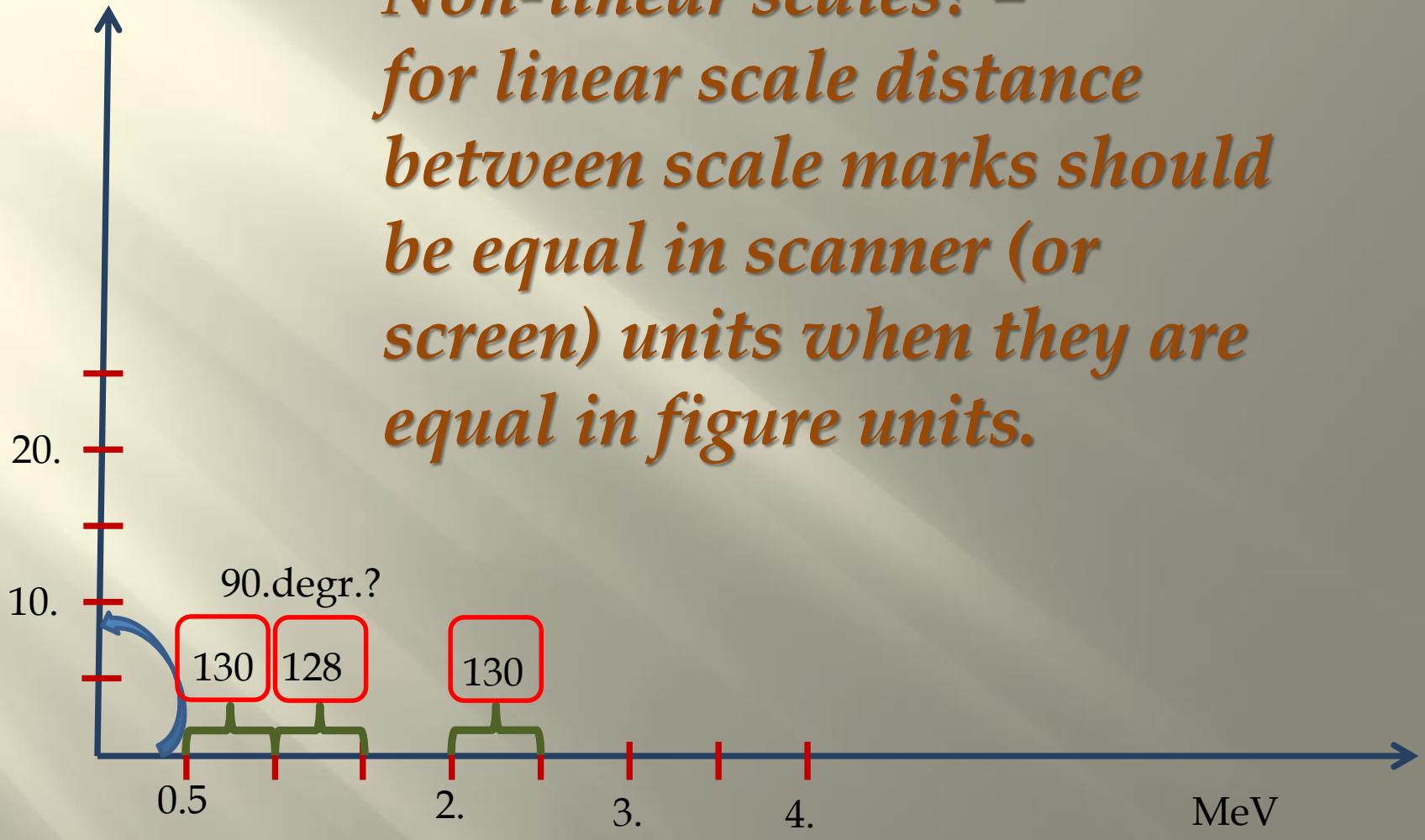

Phys.Rev,184,1217,1969 (fig.7) (00392)

PHYSICAL REVIEW VOLUME 184, NUMBER 4 20 AUGUST 1969

Elastic and Inelastic Scattering of 20.3-MeV Polarized Protons from ^{90}Zr, ^{92}Zr, and ^{92}Mo†

C. GLASHAUSSER AND R. DE SWINIARSKI,*
Service de Physique Nucléaire à Moyenne Energie, Centre d'Etudes Nucléaires, Saclay, France and Lawrence Radiation Laboratory, University of California, Berkeley, California 94720
AND
J. GOUDERGUES, R. M. LOMBARD,‡ B. MAYER, AND J. THIRION
Service de Physique Nucléaire à Moyenne Energie, Centre d'Etudes Nucléaires, Saclay, France

(Received 14 March 1969)

The elastic and inelastic scattering of polarized protons from ^{90}Zr, ^{92}Zr, and ^{92}Mo has been studied at 20.3 MeV. Asymmetries for the first 2^+ states in ^{90}Zr and ^{92}Mo are very similar; the ^{92}Zr 2^+ asymmetry is quite different from these, especially at large angles. The asymmetry for the first 3^- state in ^{92}Zr resembles the ^{90}Zr-^{92}Mo 3^- data more closely. Microscopic-model calculations for the 2^+ states with and without core-polarization contributions give poor fits to the asymmetry data, though cross sections are well fitted. Macroscopic-model calculations with the full Thomas form of the deformed spin-orbit potential give a better fit to the 2^+ data and quite closely predict the 3^- asymmetries.

I. INTRODUCTION

RECENT attempts to interpret asymmetries in the inelastic scattering of polarized protons have been only partially successful.[1–3] The predictions of the distorted-wave Born-approximation (DWBA) or coupled-channels methods were reasonably accurate for 2^+ and 3^- states in ^{56}Fe and the nickel isotopes at energies between 18.6 and 40 MeV. A macroscopic description was used; the good results were obtained only by including real, imaginary, and spin-orbit terms in the form factors. This model was unable, however, to reproduce the large asymmetries observed after excitation of the first 2^+ state in ^{52}Cr and ^{54}Fe which have 28 neutrons. (The differences between ^{54}Fe and ^{56}Fe have recently been verified at 19.6 MeV.[4]) The fact that neighboring nuclei exhibited such large differences in asymmetries suggested that a microscopic analysis was necessary. However, on the assumption of simple configurations for the states involved, the microscopic form factors closely resembled the real central part of the macroscopic form factors; neither the cross sections nor the asymmetries were well fitted.

Some of the problems in the microscopic analysis may have arisen from the neglect of collective correlations in the wave functions. Love and Satchler[5] have recently shown that core polarization (CP) can account for a large part of the cross section to states which are predominantly simple configurations. In their phenomenological model, a macroscopic-type form factor is added to the direct (D) microscopic form factor; its strength is proportional to the effective charge determined from electromagnetic decay rates. The model has been successfully applied in the analysis of differential cross sections for the excitation of 2^+ and 4^+ states in ^{90}Zr and ^{92}Zr at several energies, but it has not yet been used in the analysis of asymmetry data. Since the CP amplitude contains both imaginary and spin-orbit terms and is coherent with the D amplitude, it could produce large changes in the predicted asymmetries.

The 2^+ state in ^{90}Zr at 2.18 MeV is excited predominantly by a proton transition of the type $(1g_{9/2})_0{}^{-2}-(1g_{9/2})_2{}^{-2}$, since the neutron shell is closed. The first 2^+ state in ^{92}Mo at 1.51 MeV is also expected to be simply described in terms of $1g_{9/2}$ protons. However, the 2^+ state in ^{92}Zr is chiefly a $(2d_{5/2})^2$ neutron configuration. The 3^- state in each nucleus is strongly collective.

The macroscopic model would predict similar shapes for the differential cross sections and asymmetries for the 2^+ states and for the 3^- states in all these nuclei. On the other hand, in the microscopic model without core polarization, variations between ^{92}Zr and ^{90}Zr-^{92}Mo could arise from differences in the p-p and p-n effective interactions, and from differences in the form factors for transitions of $2d_{5/2}$ and $1g_{9/2}$ nucleons. When core polarization is included these effects are decreased, since both proton and neutron core excitations of similar types are likely to occur in all

† Work supported in part by the U. S. Atomic Energy Commission.
* NATO Fellow. Permanent address: Institut des Sciences Nucléaires, Grenoble, France.
‡ Present address: Laboratorie de Physique Atomique et Moleculaire, College de France, Paris, France.
[1] C. Glashausser, R. de Swiniarski, J. Thirion, and A. D. Hill, Phys. Rev. **164**, 1437 (1967).
[2] M. P. Fricke, E. E. Gross, and A. Zucker, Phys. Rev. **163**, 1153 (1967); V. E. Lewis, M. Calderbank, N. K. Ganguly, and M. P. Fricke, Nucl. Phys. **A117**, 673 (1968).
[3] C. Glashausser and J. Thirion, in *Advances in Nuclear Physics*, edited by M. Baranger and E. Vogt (Plenum Press, Inc., New York, 1969), Vol. II, p. 79.
[4] B. Mayer and J. Thirion (private communication).
[5] W. G. Lover and G. R. Satchler, Nucl. Phys. **A101**, 424 (1967).

and backward angles; these have been noted also at 12.7 MeV.[16] Since the 4^- state in ^{90}Zr is almost degenerate with the 3^- state, it might account for some of the large angle differences although it is unlikely to be significant at small angles. The fact that the 3^- data for ^{92}Mo and ^{90}Zr are very similar also indicates that the contribution of the 4^- state in ^{90}Zr is not important.

IV. ANALYSIS

A. Optical-Model Parameters

The optical-model parameters were determined from an analysis of the elastic cross-section and polarization data taken concurrently with the inelastic data described above. The search code MERCY, a modified version of SEEK,[17] was used. The definition of the optical potential and the search procedures employed are standard.[1] Errors on the cross sections were uniformly set at ±10%; the errors on the polarization were statistical unless these were very small. Corrections arising from the finite angular acceptance of the detectors were not included.

Good fits to the 18.6-MeV elastic scattering data for nuclei with $A\sim60$ have been obtained[18] by adopting several sets of fixed geometrical parameters for the central potential. The parameters of Perey ($r_s=r_I=1.25$ F, $a_s=0.65$ F, $a_{so}=a_I=0.47$ F) and those of Satchler ($r_s=1.24$ F, $r_I=1.28$ F, $a_s=0.65$ F, $a_I=0.50$ F, $a_{so}=0.42$ F) were about equally successful, although the latter gave better fits to the inelastic data. The spin-orbit radius r_{so} found with both sets was generally about 10% less than the real radius r_s.

These parameters were tried for the present data, but only the second set gave reasonable agreement. The average value of r_{so} was again about 10% less than r_s; the values of χ^2/N ranged from 5 to 7. Very good fits were finally obtained by searching on all parameters at once, starting from the best "Perey" and the best "Satchler" sets and several others. All initial values gave the same final results; these are listed in Figs. 6 and 7. Note that the best-fit parameters for the three nuclei are quite similar. The largest variations are observed in the value of r_{so}, but the average value is again smaller than r_s by almost 15%. The improvement in the fit with the best-fit parameters is due chiefly to the increase in a_I. This was found to be true also in the analysis of 18.8-MeV cross-section results by Gray *et al.*[14]

Attempts were made to improve these fits by introducing some volume absorption, and also by including an imaginary spin-orbit term. As expected, an increase in volume absorption reduced the surface absorption by an equivalent amount, but the quality of the fit rapidly deteriorated. On the other hand, fits almost as good as those of Figs. 6 and 7 could be obtained with an imaginary spin-orbit term of -1-

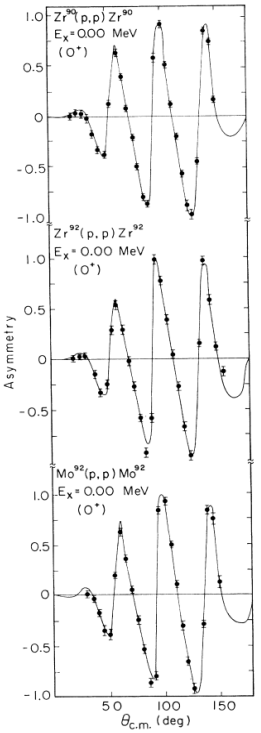

FIG. 7. Elastic-scattering asymmetries and optical-model predictions with the parameters of Table I.

[16] M. A. Melkanoff, J. Raynal, and T. Sawada, University of California at Los Angeles Report No. UCLA 66-10, 1966 (unpublished).
[17] P. Kossanyi-Demay, R. de Swiniarski, and C. Glashausser, Nucl. Phys. **A94**, 513 (1967); P. Kossanyi-Demay and R. de Swiniarski, *ibid.* **A108**, 577 (1968).

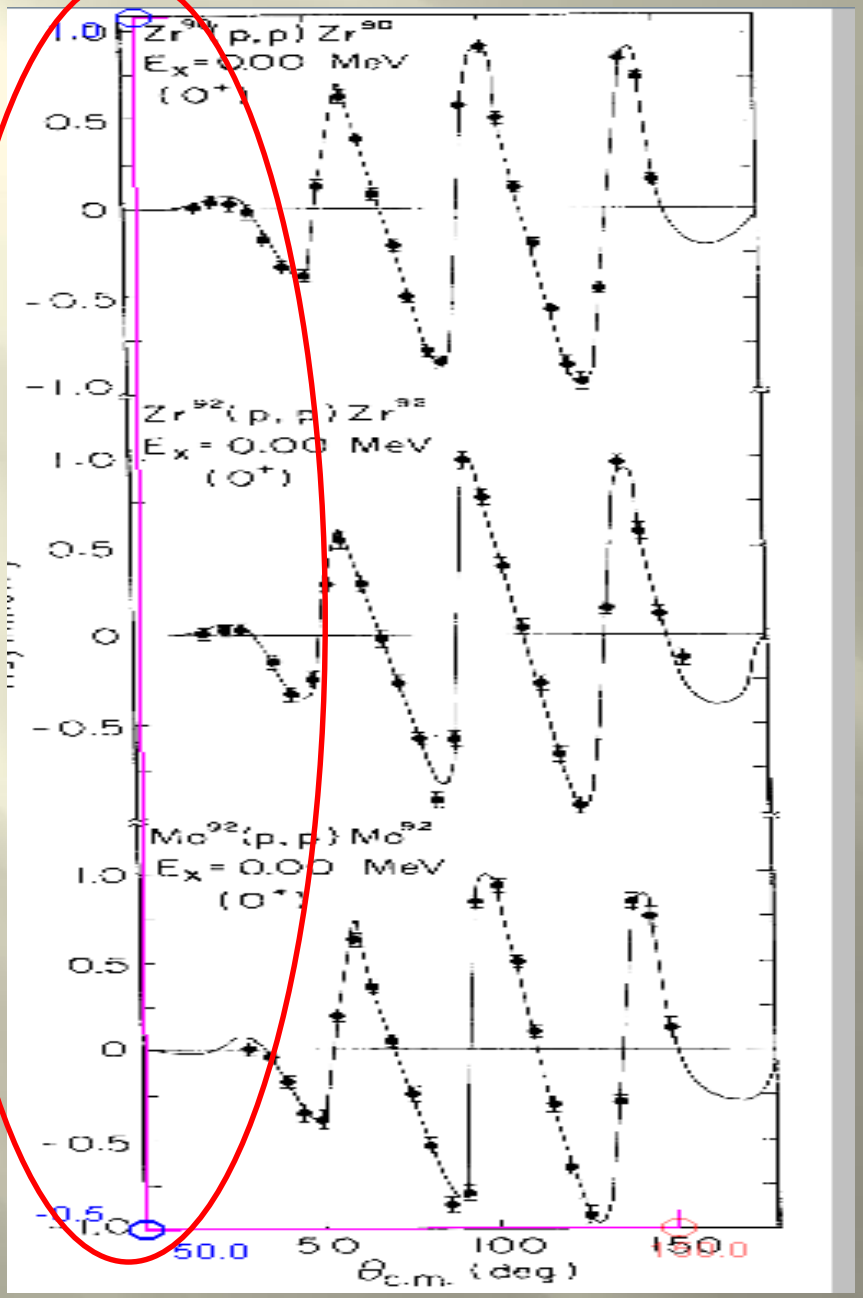

Complicated case:

angle less than 90.degr.

Set of curves with shift along ordinate

Digitization in 1997 and in 2018

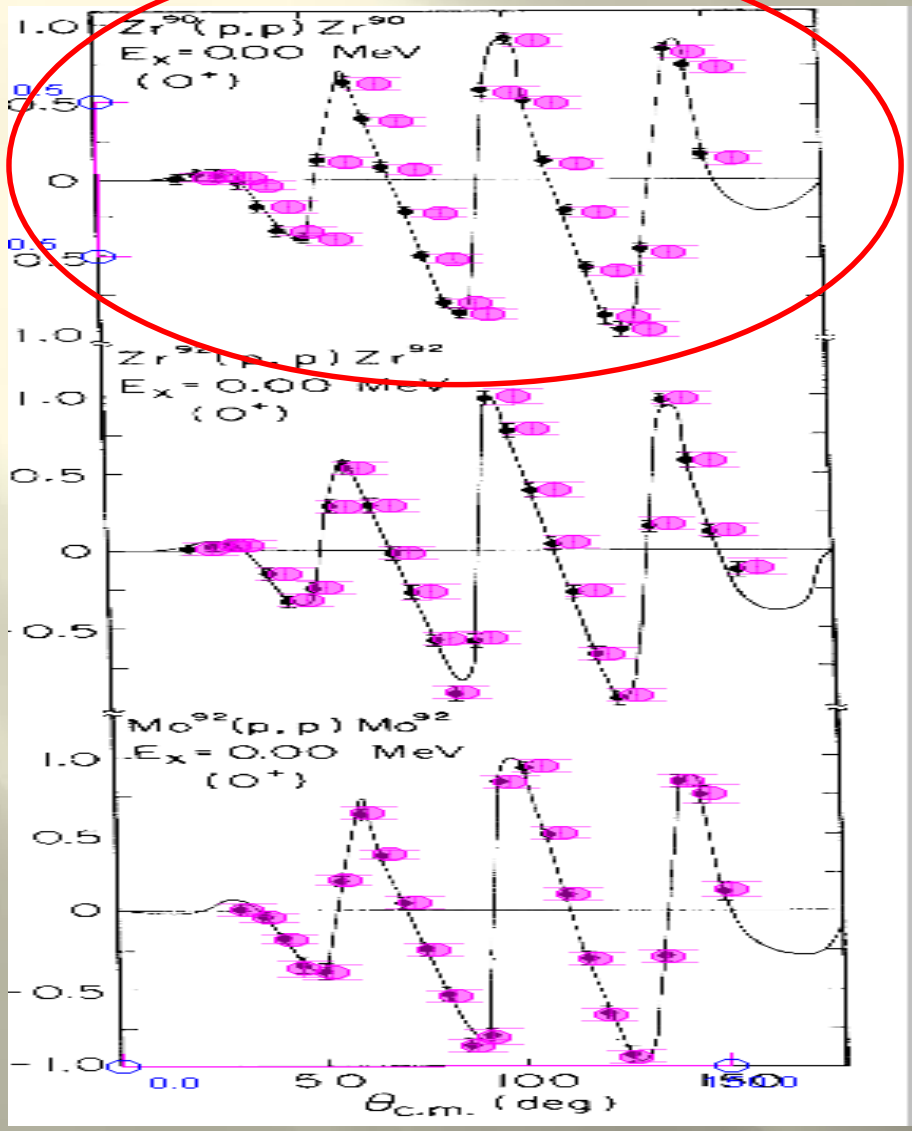

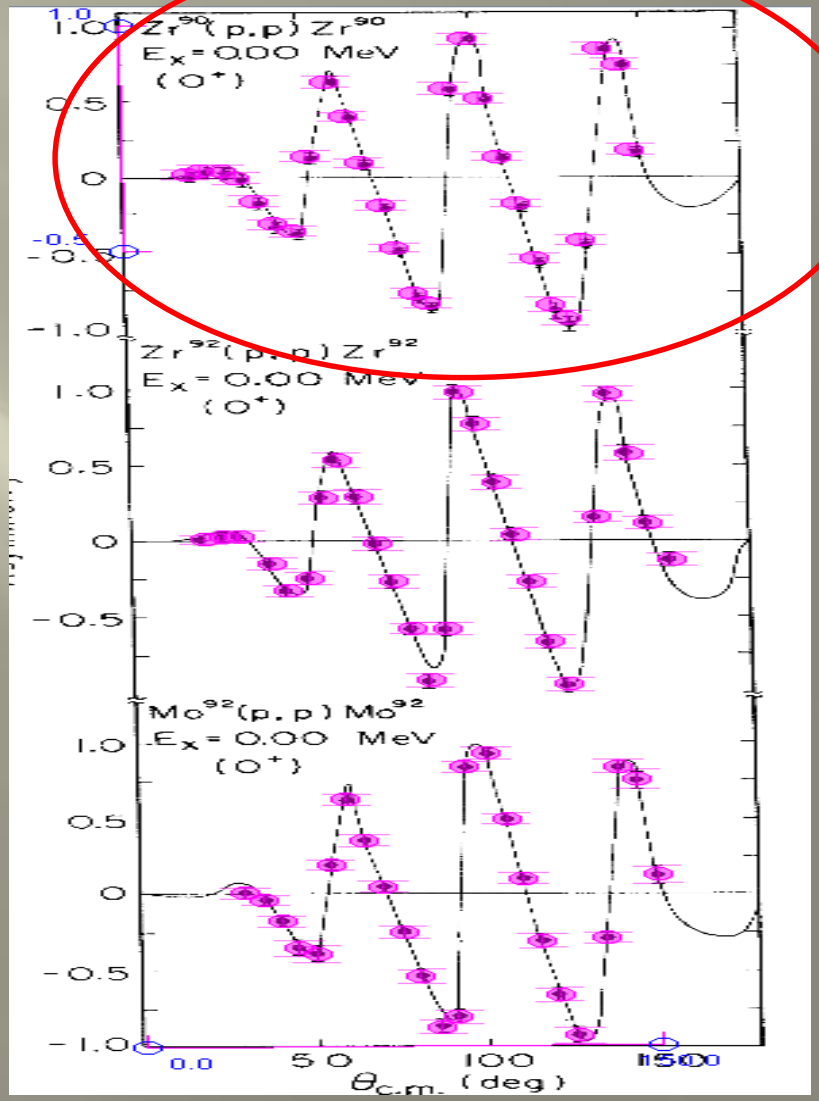

Phys.Rev,184,1217,1969 (fig.7 bottom)

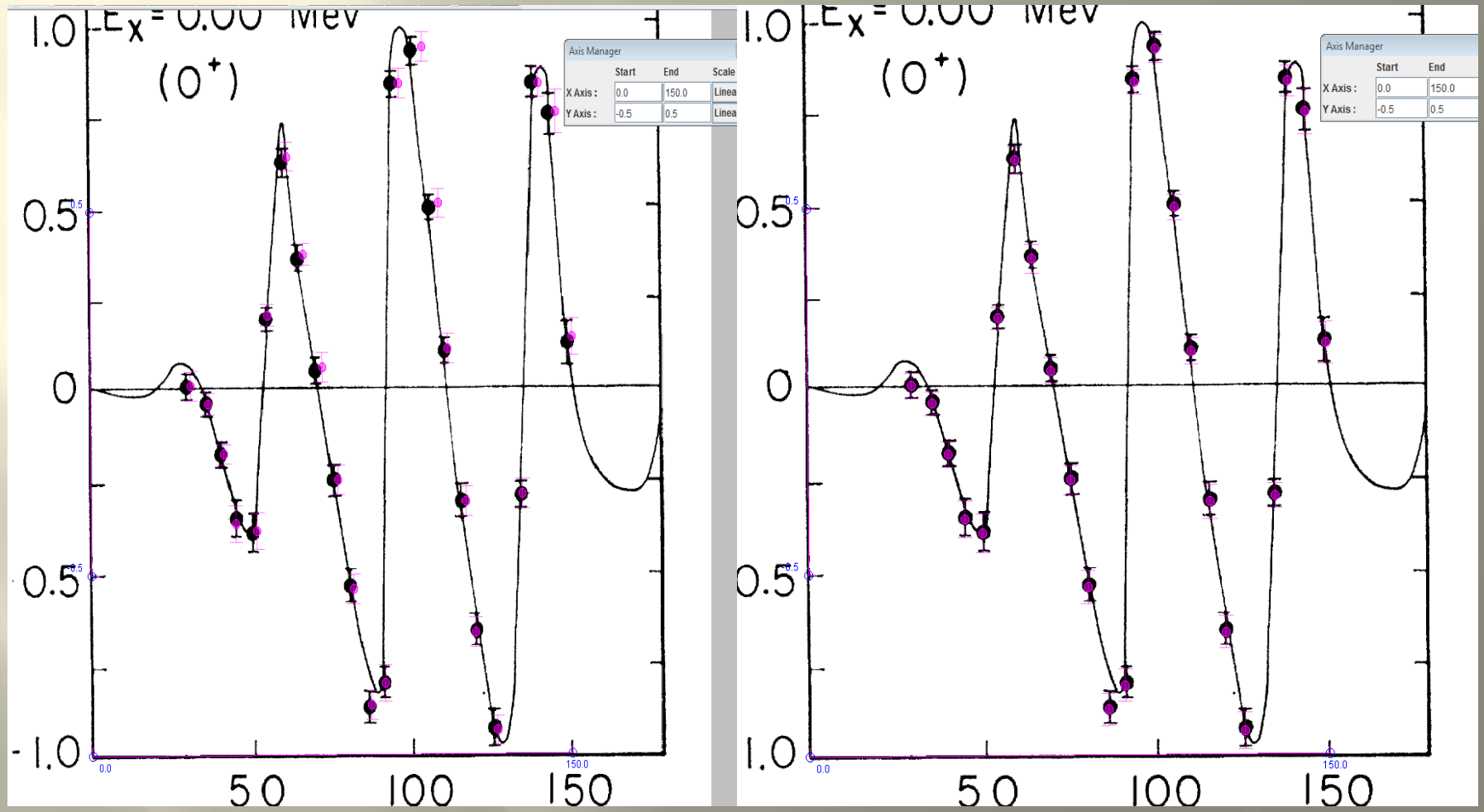

PR,184,1217,1969 (fig.7, middle)

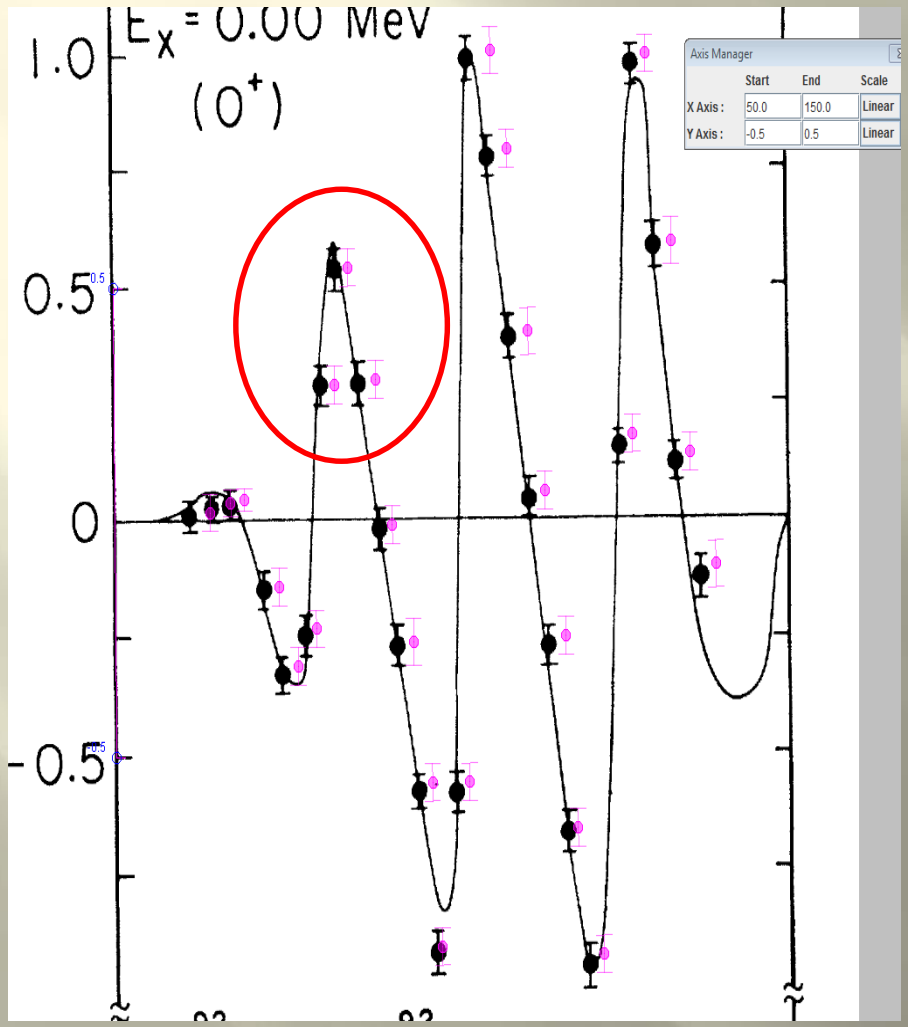

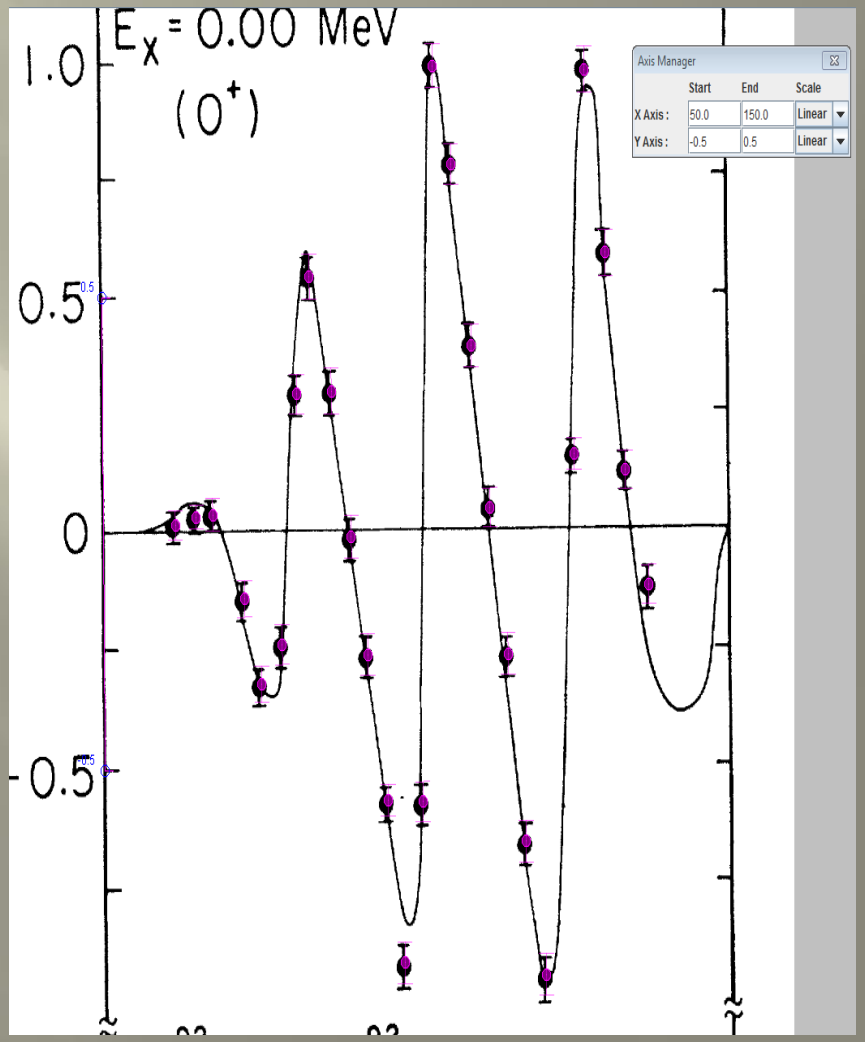

PR,184,1217,1969 (fig.7, top)

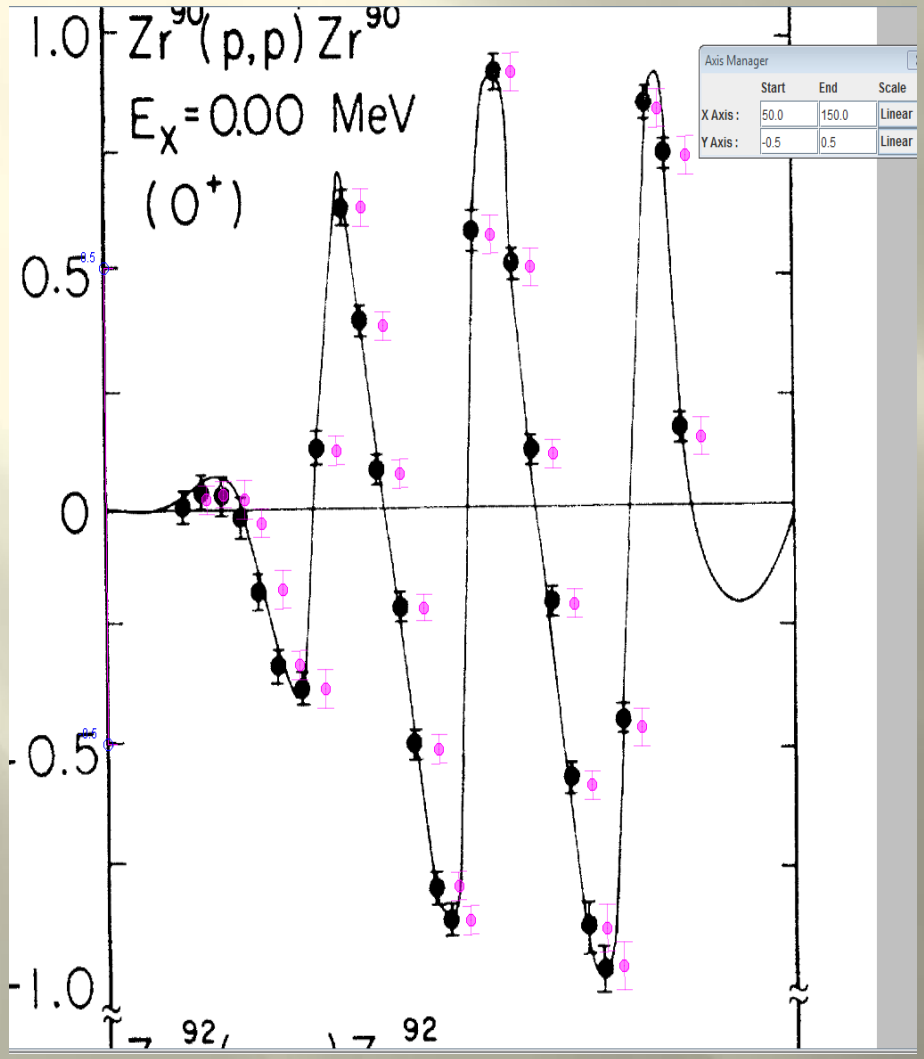

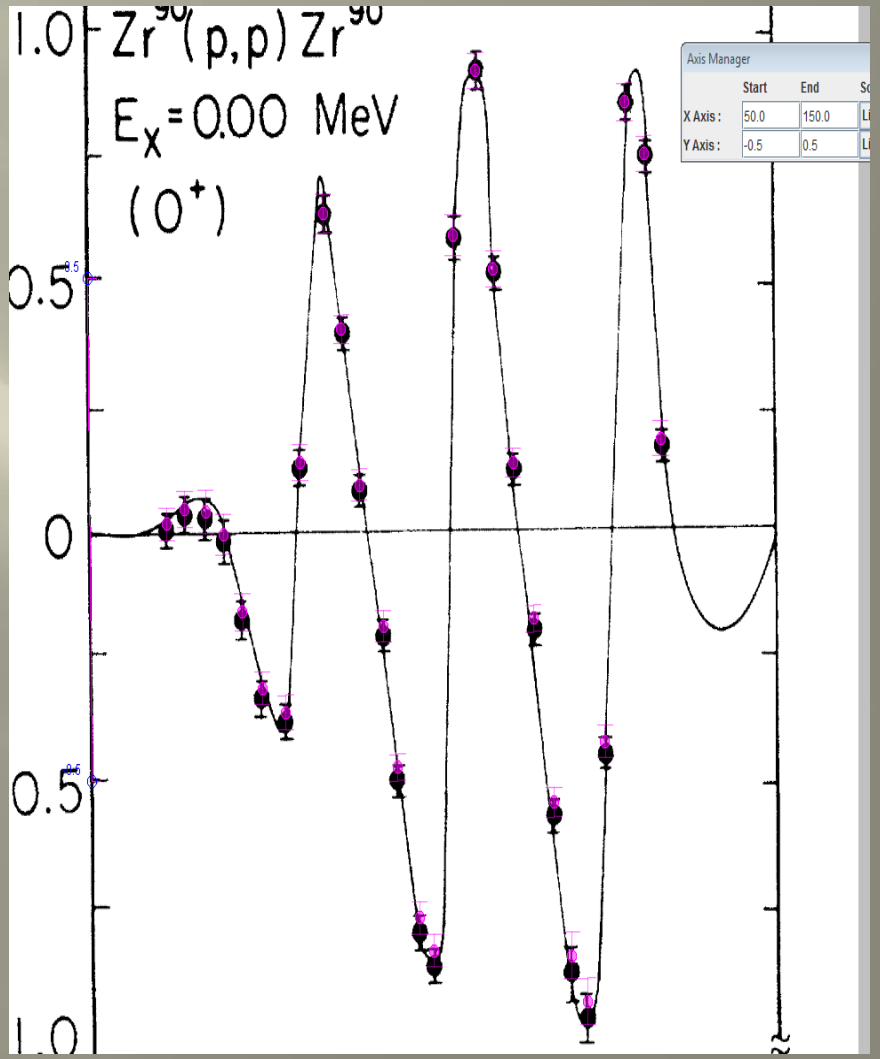

Rev.Roum.Phys.,19,653,1974 (fig.3), F0455

ELASTIC SCATTERING OF ^{3}He BY ^{9}Be AND ^{28}Si*

BY

I. BONDOUK**, Z. A. SALEH, F. MACHALI and D. A. DARWISH

Atomic Energy Establishment, Cairo, Egypt, A.R.E.

On a mesuré des sections efficaces différentielles de diffusion élastique du ^{3}He sur ^{9}Be et ^{28}Si, dans l'intervalle d'énergies incidentes de 1,20 MeV÷2,50 MeV, pour quatre angles de diffusion.

Dans le cas de la réaction ^{9}Be(^{3}He, ^{2}He)^{3}Be les sections efficaces ont une allure lisse et ne montrent aucun comportement de résonance.

Les distributions angulaires ont été mesurées pour des angles compris entre 60° et 150° (système du laboratoire) avec un pas de 200 KeV, entre 1,6÷2,4 MeV. Les données ont été analysées à l'aide du modèle optique. Un bon fit a été obtenu en utilisant un potentiel d'absorption de surface.

Les sections efficaces de la réaction ^{28}Si(^{3}He, ^{3}He)^{28}Si suivent le comportement des sections efficaces Rutherford dans tout le domaine des énergies incidentes.

Differential cross-sections for the elastic scattering of ^{3}He from ^{9}Be and ^{28}Si have been measured in the $E_{He^3} = 1.20 \div 2.50$ MeV region at four scattering angles. The ^{9}Be (^{3}He, ^{3}He)^{9}Be cross-sections are smooth over the entire energy range and show no clear resonance behaviour. Angular distributions from 60° to 150° (Lab) were measured in 200 KeV steps from 1.60 to 2.40 MeV and optical model analysis of these data were made. Good fits were obtained with a surface absorption potential. The ^{28}Si(^{3}He, ^{3}He) ^{28}Si cross-sections follow the Rutherford cross-sections in the entire energy range.

1. INTRODUCTION

In recent years many ^{3}He elastic scattering experiments and analyses in terms of the optical model have been carried out [1]. However for light nuclei ($A < 16$) few such studies have been published [2] [6]. The systematic study of the optical potential for ^{3}He is important not only as a description of the elastic process itself, but also for the need of accu-

* Received January 15, 1974

** I A E A. fellowship at the Institute of Atomic Physics – Bucharest – Romania

4. RESULTS AND DISCUSSIONS

A. ^{9}Be(^{3}He, ^{3}He)^{9}Be

The elastic scattering of ^{3}He by ^{9}Be has been measured at four angles $\theta_{c.m.} = 98$, 122, 137 and 145° in steps of 20 KeV in the bombarding ^{3}He energy range $E_{He^3} = 1.20 \div 2.40$ MeV. Fig. 3 shows a plot of the

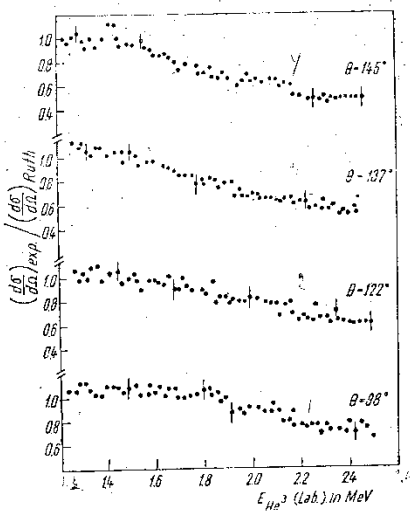

Fig. 3. — The ratio of the experimental differential cross-section of the ^{9}Be(^{3}He, ^{3}He)^{9}Be reaction to the Rutherford cross-section at four centers of mass angles as a function of the energy.

$\sigma_{exp}/\sigma_{Rath}$ ratio between the measured cross-section σ_{exp} and the Rutherford cross-section as a function of ^{3}He energy. The excitation functions are smooth over the entire energy range and show no clear resonance behaviour. The absence of any resonance behaviour in the cross-section may be explained by the fact that the excitation energy of the C^{12} compound nucleus was about 28 MeV in the energy range considered. At this excitation energy any isolated resonance behaviour is improbable.

Angular distributions have been measured for five energies from 1.60 to 2.40 MeV in steps of 200 KeV for lab. angles from 60° to 150°. The monitor was placed at 150° to the beam direction and was used to normalize the intensity of the scattered ^{3}He at every angle.

The optimum parameters obtained from the four parameter searches over U_R, W_D, a_R and a_I using surface absorption without spin-orbit coupling are listed in Table 1 with the χ^2-values and σ_R, the calculated

Digitization in 1986 and in 2018 (fig.3)

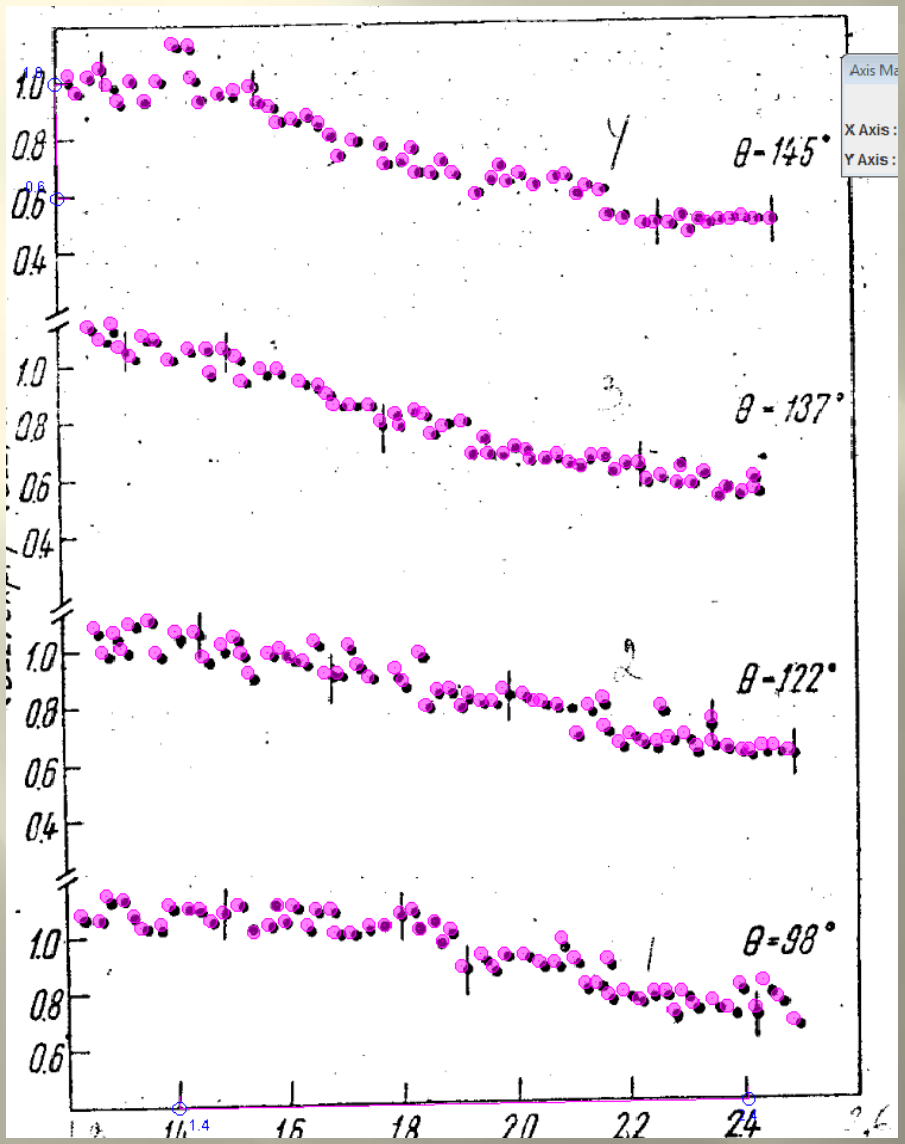

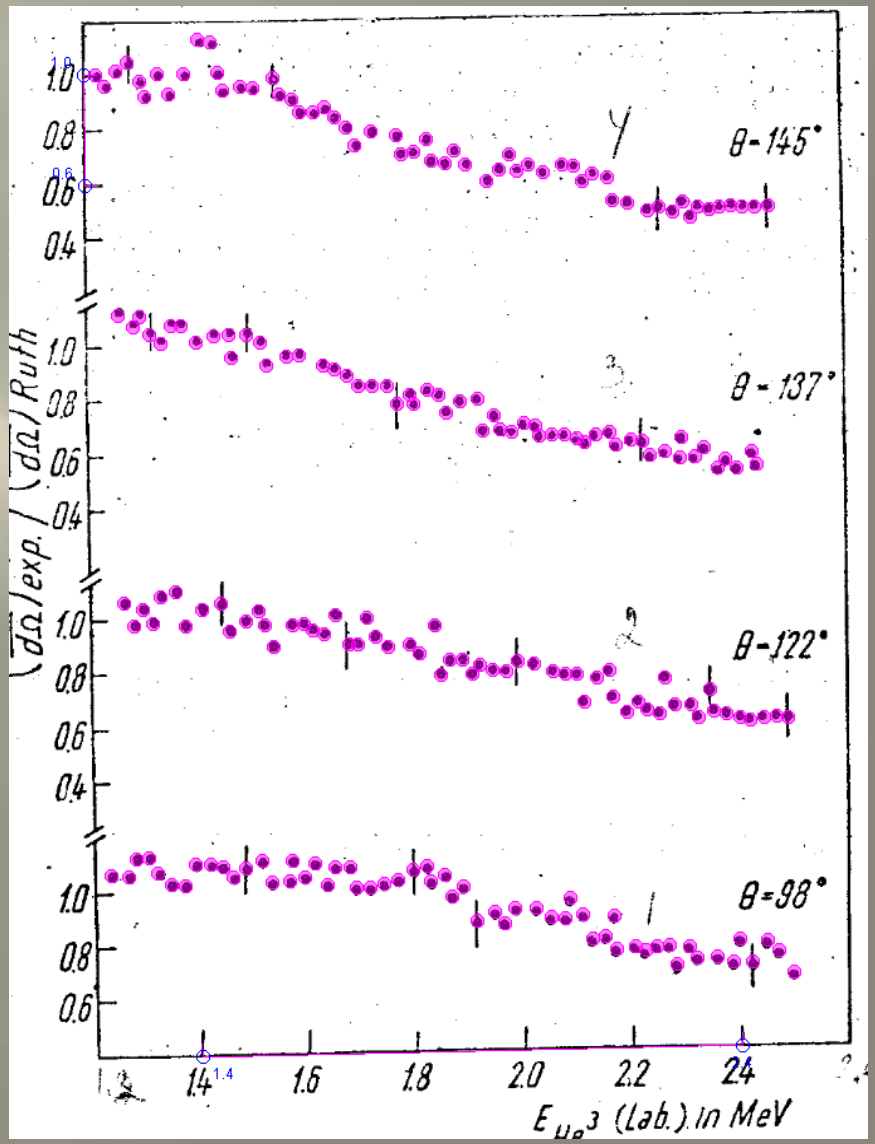

Rev.Roum.Phys.,19,653,1974 (F0455)

ELASTIC SCATTERING OF ^{3}He BY ^{9}Be AND ^{28}Si*

BY

I. BONDOUK**, Z. A. SALEH, F. MACHALI and D. A. DARWISH

Atomic Energy Establishment, Cairo, Egypt, A.R.E.

On a mesuré des sections efficaces différentielles de diffusion élastique du ^{3}He sur ^{9}Be et ^{28}Si, dans l'intervalle d'énergies incidentes de 1,20 MeV÷2,50 MeV, pour quatre angles de diffusion.

Dans le cas de la réaction ^{9}Be(^{3}He, ^{3}He)^{9}Be les sections efficaces ont une allure lisse et ne montrent aucun comportement de résonance.

Les distributions angulaires ont été mesurées pour des angles compris entre 60° et 150° (système du laboratoire) avec un pas de 200 KeV, entre 1,6÷2,4 MeV. Les données ont été analysées à l'aide du modèle optique. Un bon fit a été obtenu en utilisant un potentiel d'absorption de surface.

Les sections efficaces de la réaction ^{28}Si(^{3}He, ^{3}He)^{28}Si suivent le comportement des sections efficaces Rutherford dans tout le domaine des énergies incidentes.

Differential cross-sections for the elastic scattering of ^{3}He from ^{9}Be and ^{28}Si have been measured in the $E_{He3} = 1.20 \div 2.50$ MeV region at four scattering angles. The ^{9}Be(^{3}He, ^{3}He)^{9}Be cross-sections are smooth over the entire energy range and show no clear resonance behaviour. Angular distributions from 60° to 150° (Lab) were measured in 200 KeV steps from 1.60 to 2.40 MeV and optical model analysis of these data were made. Good fits were obtained with a surface absorption potential. The ^{28}Si(^{3}He, ^{3}He) ^{28}Si cross-sections follow the Rutherford cross-sections in the entire energy range.

1. INTRODUCTION

In recent years many ^{3}He elastic scattering experiments and analyses in terms of the optical model have been carried out [1]. However for light nuclei ($A < 16$) few such studies have been published [2] [6]. The systematic study of the optical potential for ^{3}He is important not only as a description of the elastic process itself, but also for the need of accu-

* Received January 15, 1974

** I A E A. fellowship at the Institute of Atomic Physics – Bucharest – Romania

reaction cross-sections. In general, the best fits at all energies were obtained with this set. For example, at 1.80 MeV, the χ^2 values were :

(i) 76.2 for volume absorption without spin-orbit coupling,

(ii) 6.966 for surface absorption without spin-orbit coupling.

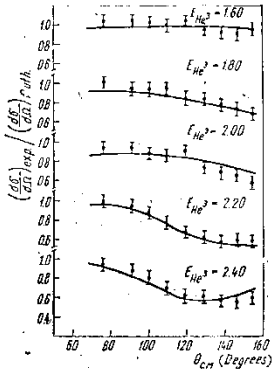

Fig. 4. – Angular distributions for ^{9}Be(^{3}He, ^{3}He)^{9}Be reaction plotted as the ratio of the experimental differential cross-section to the Rutherford cross-section. The solid curves give the optical model fits with the parameters given in Table 1.

The variation of r_{oR}, r_{oI} and r_{oC} did not improve the fits and no better fits were obtained by the inclusion of spin orbit interaction.

The calculated elastic scattering cross-sections using surface absorption without spin-orbit coupling are compared with the experimental data in Fig. 4. It is seen that a good agreement is obtained.

Table 1

E_{He^3}(MeV)	1.60	1.80	2.0	2.20	2.40
U_R(MeV)	191.0	150.0	137.153	167.976	170.630
W_D(MeV)	14.60	14.60	14.60	14.60	14.60
a_R(fm)	0.4040	0.7008	0.7350	0.5987	0.6223
a_I(fm)	0.7420	0.5799	0.6058	0.4440	0.4977
σ_R(mb/sr)	82.99	229.99	307.82	291.10	333.80
χ^2	13.200	6.996	30.110	3.029	21.940

B. ^{28}Si(^{3}He, ^{3}He)^{28}Si

The yield of elastically scattered ^{3}He from ^{28}Si was measured at the two scattering angles $\theta_{c.m} = 90°$ and $\theta_{c.m} = 125°$ for the ^{3}He energy range 1.40÷2.50 MeV. Excitation functions obtained are shown in Fig. 5.

Digitization in 1986 and in 2018 (fig.4)

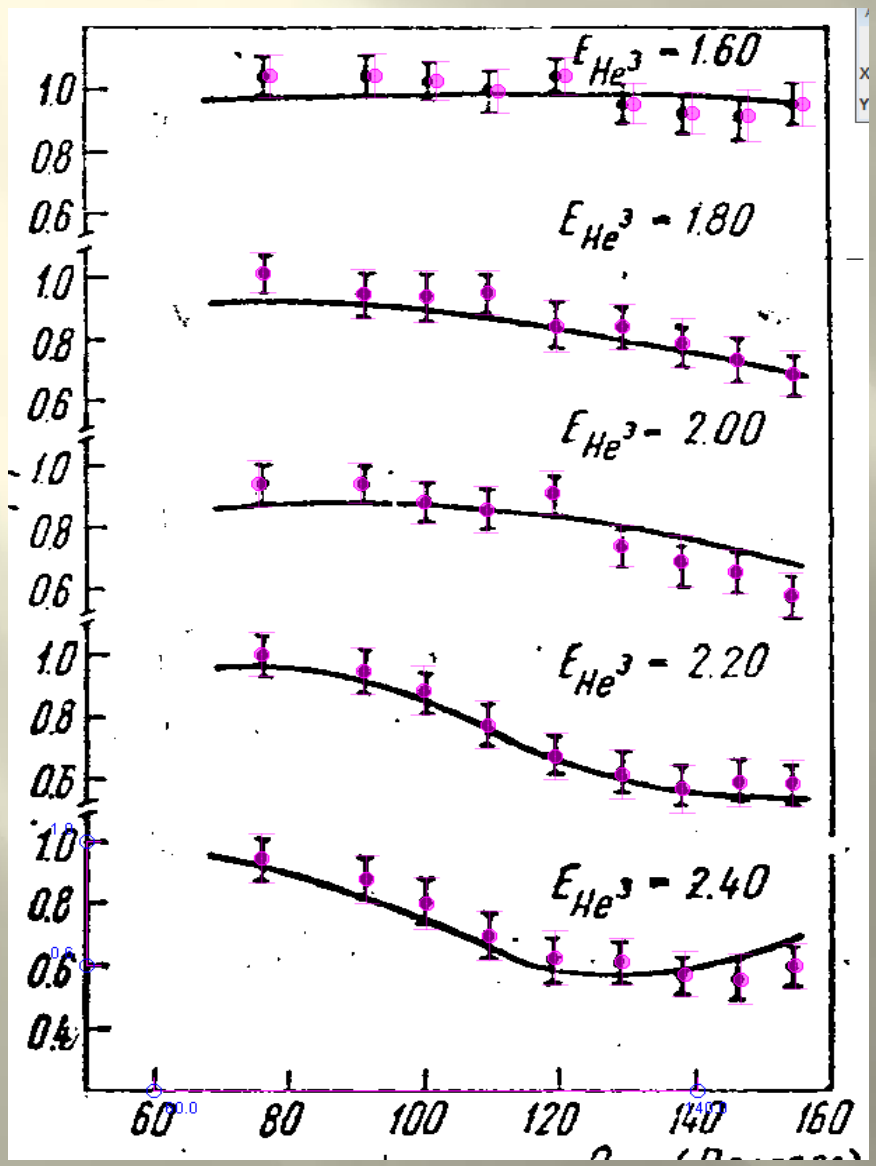

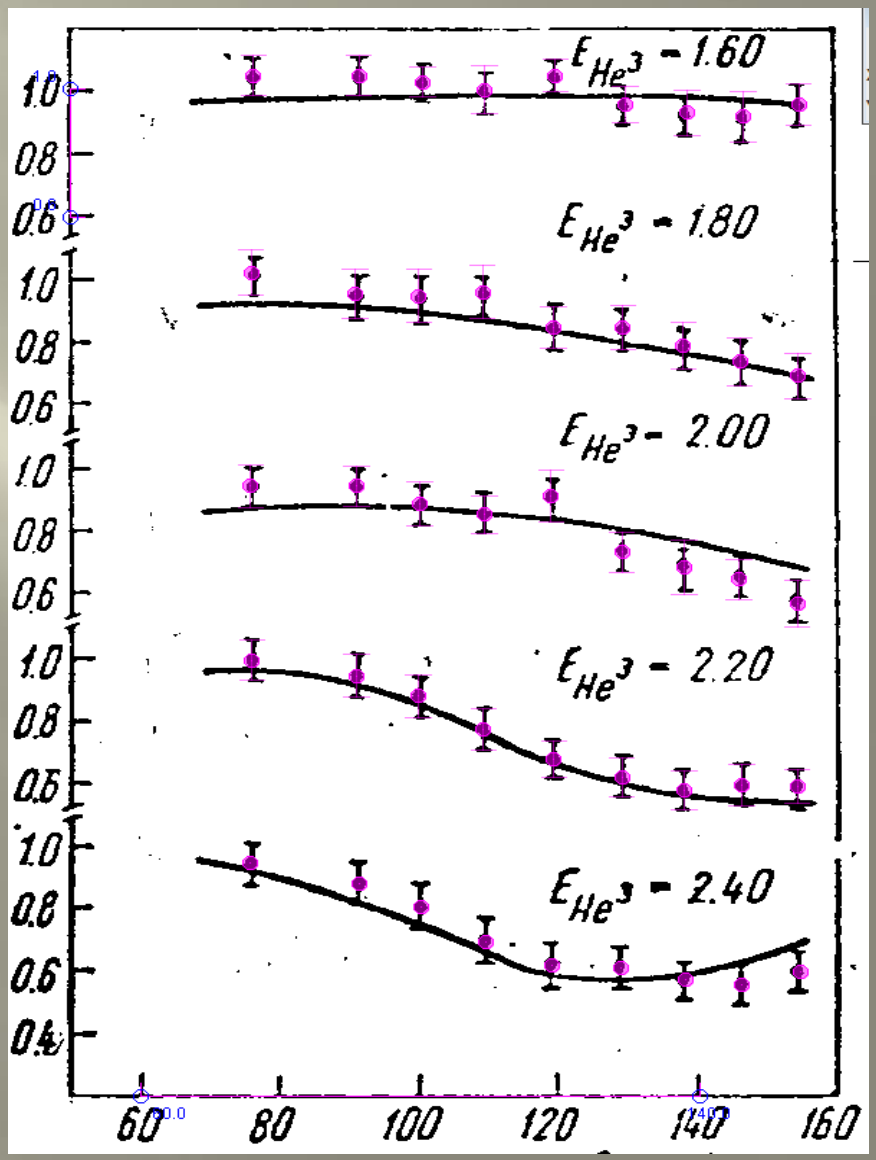

Rev.Roum.Phys.,19,653,1974, (fig.5), F0455

ELASTIC SCATTERING OF ^{3}He BY ^{9}Be AND ^{28}Si*

BY

I. BONDOUK**, Z. A. SALEH, F. MACHALI and D. A. DARWISH

Atomic Energy Establishment, Cairo, Egypt, A.R.E.

On a mesuré des sections efficaces différentielles de diffusion élastique du ^{3}He sur ^{9}Be et ^{28}Si, dans l'intervalle d'énergies incidentes de 1,20 MeV÷2,50 MeV, pour quatre angles de diffusion.

Dans le cas de la réaction ^{9}Be(^{3}He, ^{3}He)^{3}Be les sections efficaces ont une allure lisse et ne montrent aucun comportement de résonance.

Les distributions angulaires, ont été mesurées pour des angles compris entre 60° et 150° (système du laboratoire) avec un pas de 200 KeV, entre 1.6÷2,4 MeV. Les données ont été analysées à l'aide du modèle optique. Un bon fit a été obtenu en utilisant un potentiel d'absorption de surface.

Les sections efficaces de la réaction ^{28}Si(^{3}He, ^{3}He)^{28}Si suivent le comportement des sections efficaces Rutherford dans tout le domaine des énergies incidentes.

Differential cross-sections for the elastic scattering of ^{3}He from ^{9}Be and ^{28}Si have been measured in the E_{He^3} = 1.20÷2.50 MeV region at four scattering angles. The ^{9}Be (^{3}He, ^{3}He)^{9}Be cross-sections are smooth over the entire energy range and show no clear resonance behaviour. Angular distributions from 60° to 150° (Lab) were measured in 200 KeV steps from 1.60 to 2.40 MeV and optical model analysis of these data were made. Good fits were obtained with a surface absorption potential. The ^{28}Si(^{3}He, ^{3}He) ^{28}Si cross-sections follow the Rutherford cross-sections in the entire energy range.

1. INTRODUCTION

In recent years many ^{3}He elastic scattering experiments and analyses in terms of the optical model have been carried out [1]. However for light nuclei ($A < 16$) few such studies have been published [2]–[6]. The systematic study of the optical potential for ^{3}He is important not only as a description of the elastic process itself, but also for the need of accu-

* Received January 15, 1974

** I A E A. fellowship at the Institute of Atomic Physics – Bucharest – Romania

The cross-section is seen to follow the Rutherford value up to an energy of 2.50 MeV. This behaviour is attributed to the high coulomb barrier [~ 7.0 MeV] in this case.

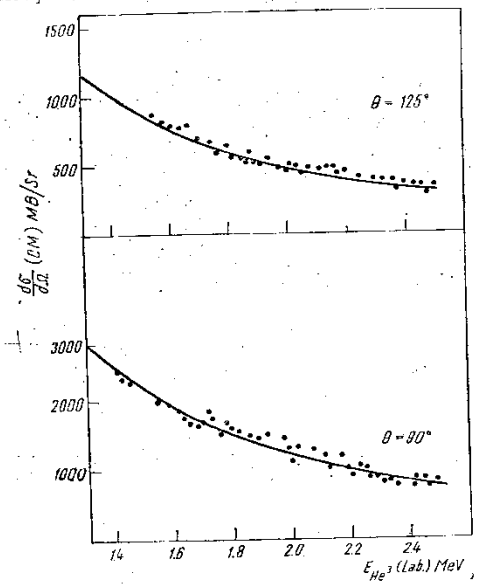

Fig. 5. — Differential cross-sections for ^{28}Si(^{3}He, ^{3}He)^{28}Si reaction as a function incident ^{3}He energy at two centers of mass angles. The solid lines represent the Rutherford cross-sections.

5. CONCLUSIONS

The present analysis of the ^{9}Be (^{3}He, ^{3}He)^{9}Be shows the adequacy of the optical model in describing the elastic scattering of ^{3}He by light nuclei at low energies. Good fits were obtained with surface absorption. The inclusion of the spin-orbit interaction did not essentially improve the fits. Parameters found in the present analysis are physically reasonable. DWBA calculations of low energy reactions involving ^{3}He particles and ^{9}Be based on these optical model parameters are in progress.

Digitization in 1986 and in 2018 (fig.5)

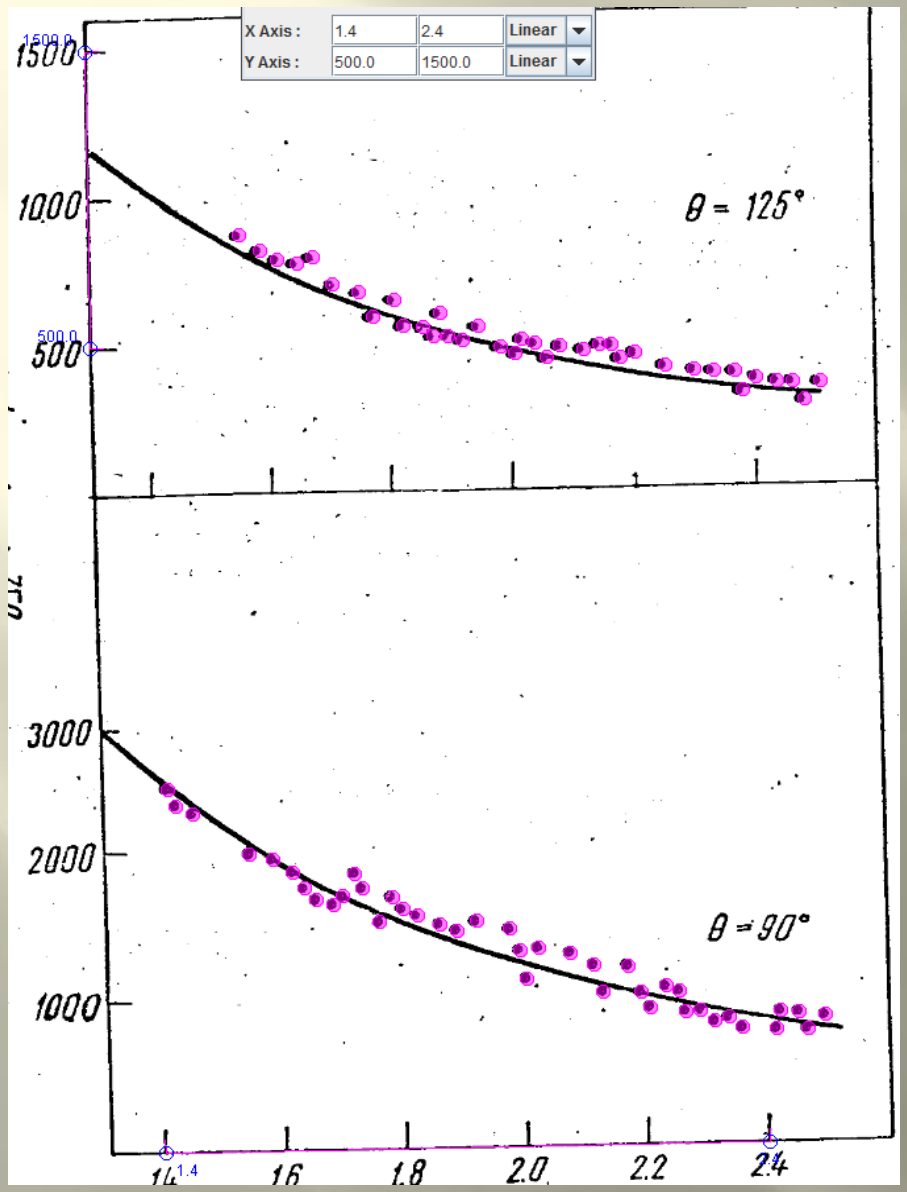

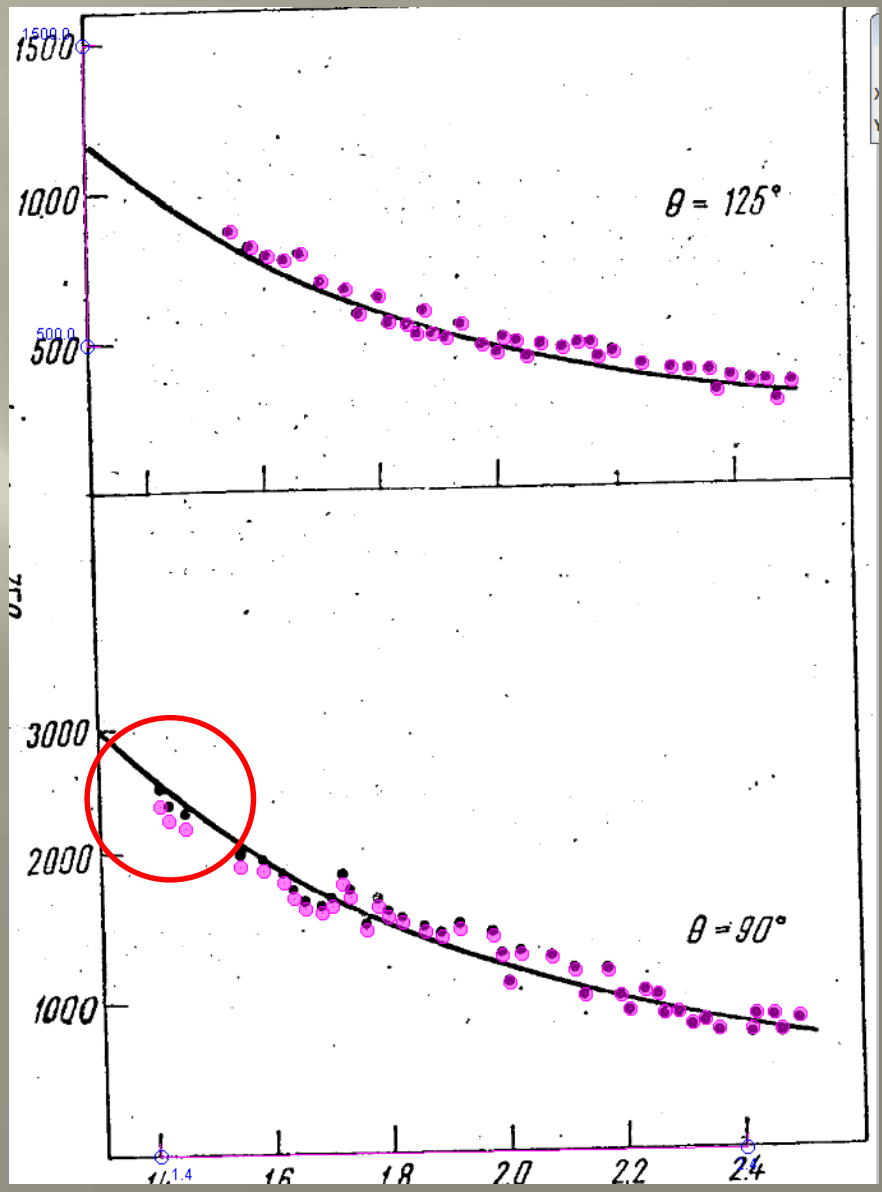

Different visualization using GSYS of last digitization of fig.5 (bottom).

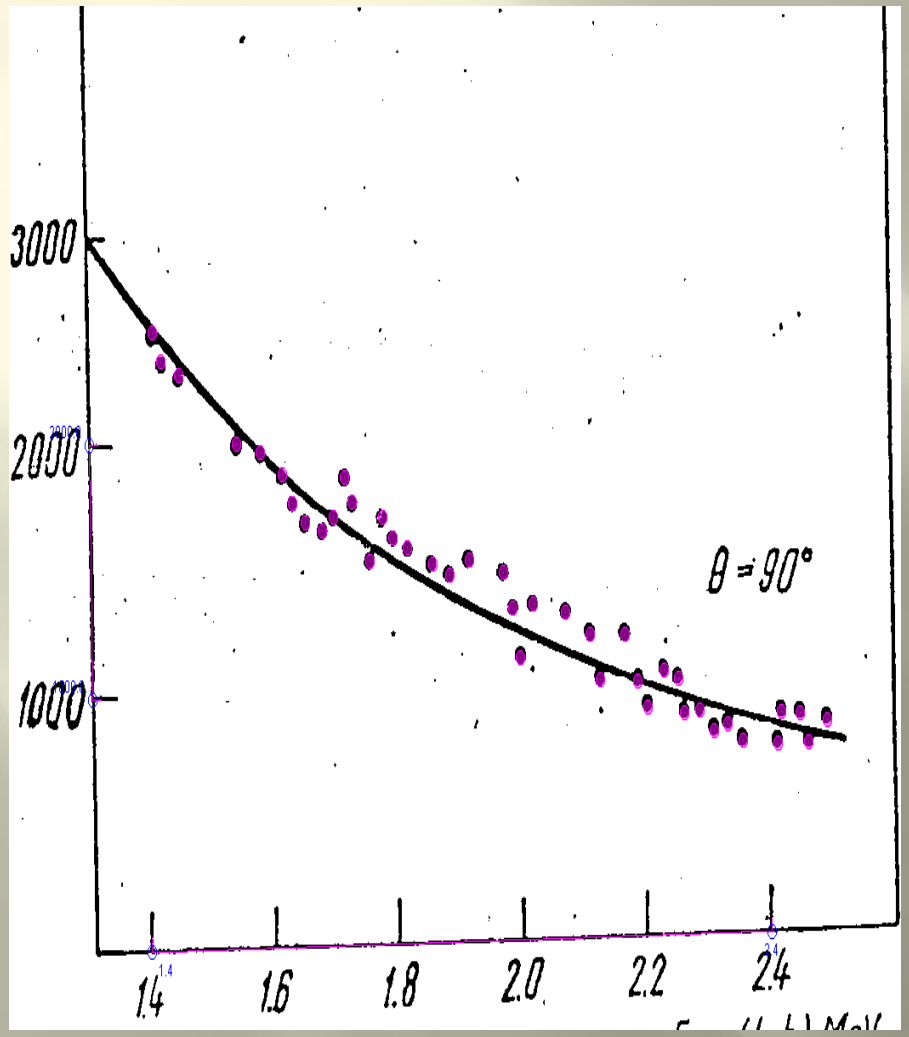

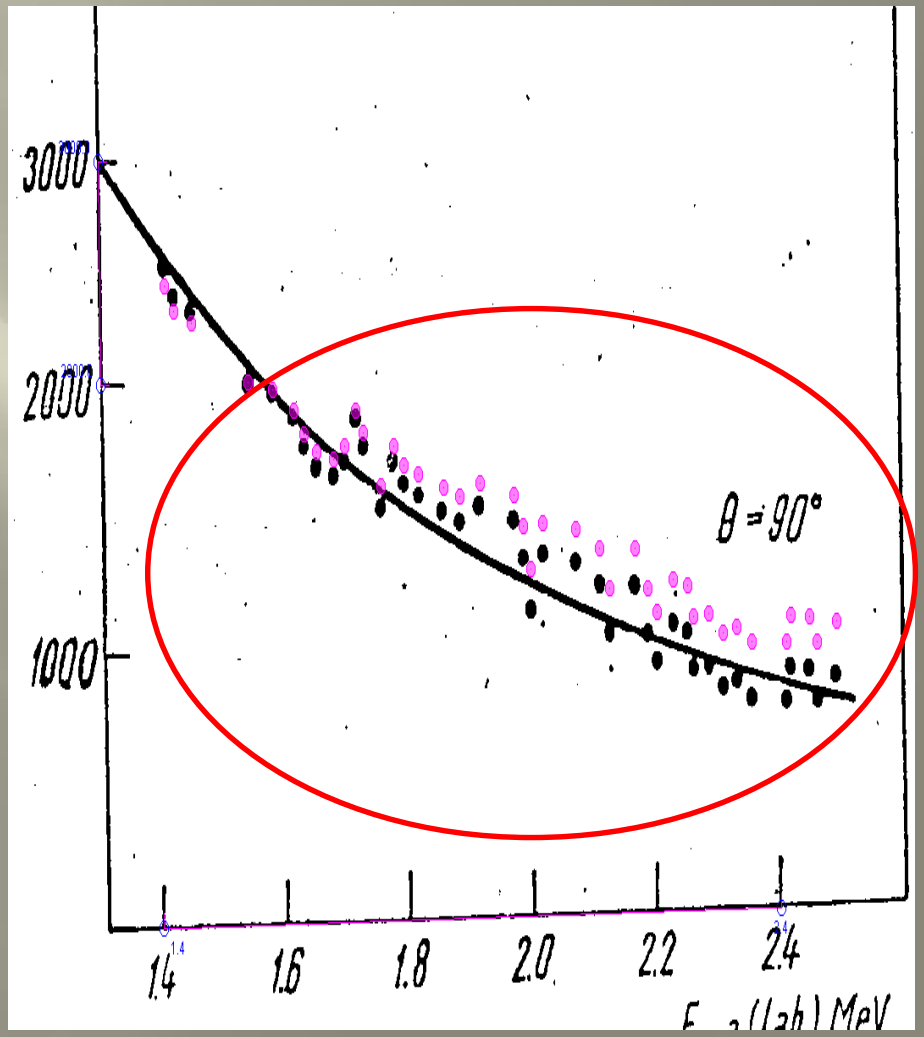

Appl.Rad.Isot. 34,1425,1983 (A0234, fig.3)

Int. J. Appl. Radiat. Isot. Vol. 34, No. 10, pp. 1425–1430, 1983
Printed in Great Britain.

0021-9681/83 $3.00 + 0.00

Excitation Functions of Deuteron Induced Nuclear Reactions On Natural Tellurium and Enriched ^{122}Te: Production of ^{123}I via the ^{122}Te(d,n)^{123}I-Process

J. H. ZAIDI*, S. M. QAIM and G. STÖCKLIN

Institut für Chemie 1 (Nuklearchemie), Kernforschungsanlage Jülich GmbH, D-517 Jülich, FRG

(Received 26 October 1982, in revised form 17 January 1983)

Excitation functions were measured by the stacked foil technique for (d,xn) reactions on natural tellurium up to $E_d \approx 14$ MeV as well as for (d,xn) and some other reactions on 96.45% enriched ^{122}Te up to $E_d = 35$ MeV. Thick target yields were calculated for the formation of ^{121}I, ^{122}I and ^{123}I. The optimum energy range for the production of ^{123}I via the ^{122}Te(d,n)^{123}I reaction is $E_d = 14 \rightarrow 8$ MeV, and the theoretical thick target yield 1.7 mCi/μAh. The practical yield for a compact cyclotron with an on-target energy of 12.7 MeV is only 0.5 mCi/μAh. Using a high-current target system and separation of radioiodine via dry distillation, batch yields of 60 mCi ^{124}I are obtained. The level of ^{124}I-impurity at EOB is 0.08%. However, about 1.50% ^{126}I is also formed. A comparison of the three direct methods of production of ^{123}I, viz. ^{124}Te(p,2n)^{123}I, ^{123}Te(p,n)^{123}I and ^{122}Te(d,n)^{123}I reactions, is given. The (d,n) reaction is most suitable as far as the ^{124}I-impurity level is concerned. The significantly higher yields of the (p,2n) process, however, may still justify the use of that reaction for large scale production of ^{123}I.

Introduction

Due to its suitable physical properties ^{123}I is considered to be one of the best radionuclides for *in-vivo* diagnostic nuclear medical studies using conventional γ-cameras or single photon emission computed tomography. For its production about 25 nuclear processes have been suggested (for reviews cf. Refs 1–5). All those processes, however, can be grouped under two general headings:

(i) indirect methods, i.e. those which make use of the

$$^{123}\text{Xe} \xrightarrow{\frac{1.9\,\text{h}}{2.0\,\text{h}}} {}^{123}\text{I}$$ precursor system.

(ii) direct methods.

The ^{123}Xe–^{123}I precursor method demands the use of medium to high energy machines and gives rise to high-purity ^{123}I, the *major impurity* being 60 d ^{125}I (0.2–0.5%). For routine and large scale production of ^{123}I the ^{127}I(p,5n)^{123}Xe, ^{127}I(d,6n)^{123}Xe and Cs,La(p,spall)^{123}Xe processes are generally used.

The direct methods of production of ^{123}I require low to medium energy cyclotrons and in general consist of proton and deuteron induced nuclear reactions on enriched tellurium isotopes. Out of the three major reactions, namely ^{124}Te(p,2n)^{123}I, ^{123}Te(p,n)^{123}I and ^{122}Te(d,n)^{123}I, the (p,2n) reaction has been most extensively investigated. It is a high-yield reaction but the level of the ^{124}I-impurity precludes its wide-spread use for production purposes. The other two reactions have not been investigated in detail.

The ^{122}Te(d,n)^{123}I reaction appeared promising to us. A few reports on the use of this reaction exist.[6–8] However, no detailed study, especially on cross section measurements, has been reported.

Excitation Functions

Excitation functions were measured by the conventional stacked foil technique. Since tellurium foils are not commercially available, an electroplating method was developed to obtain thin tellurium samples. The effect of various parameters, such as concentration, current density etc., were studied and the following conditions found to be most suitable: 0.1 M Te solution in 2.0 M HCl, current density 1.5 mA/cm^2, electroplating time 2–3 h. Titanium foils

*IAEA Fellow, on leave from Pakistan Institute of Nuclear Science and Technology, Rawalpindi, Pakistan.

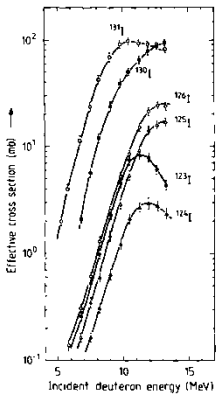

Fig. 1. Excitation functions for the formation of ^{123}I, ^{124}I, ^{125}I, ^{126}I, ^{130}I and ^{131}I in the interactions of deuterons with natural tellurium.

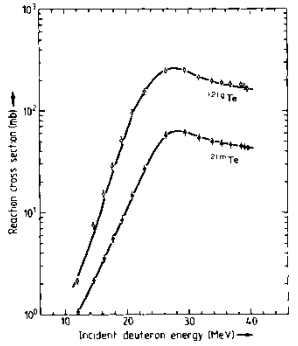

Fig. 3. Excitation functions for the formation of ^{121g}Te and ^{121m}Te in the interactions of deuterons with 96.45% enriched ^{122}Te. The contributing processes are (d,p2n), (d,dn) and (d,t).

CV 28 and the medium energy machine JULIC. The transition from the low energy data (CV 28) to medium energy data (JULIC) is excellent. The magnitudes and shapes of the three excitation functions reported here are similar to those for the (d,xn) reactions on ^{121}I (cf. Ref. 13). The threshold of the (d,3n) reaction is rather high so that use of a deuteron beam from a compact cyclotron would not give rise to ^{122}I. Some contamination from ^{122}I is to be expected. However, since its half-life is only 3.6 min its contribution after half an hour is negligible. The optimum energy range for the production of ^{123}I via the ^{122}Te(d,n)^{123}I reaction at a compact cyclotron is 14→8 MeV.

Excitation functions for the formation of some radioisotopes of tellurium and antimony, in the interactions of deuterons with enriched ^{122}Te, were also measured. The cross section data for the formation of ^{121m}Te and ^{121g}Te are shown in Fig. 3. ^{121m}Te decays independently to ^{121}Sb and contributes <0.03% to the formation of ^{121g}Te. The curves are rather complex and include contributions from (d,p2n), (d,dn) and (d,t) processes.

Figure 4 shows the excitation functions of ^{122}Te(d,p)^{123m}Te and ^{122}Te(d,α)^{120g}Sb reactions. In the latter case only the longer-lived isomeric state of ^{120}Sb

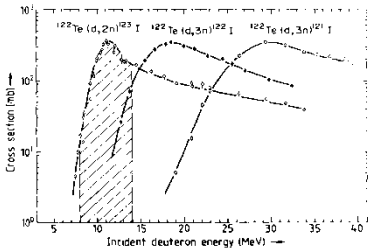

Fig. 2. Excitation functions of (d,xn) reactions on 96.45% enriched ^{122}Te.

Digitization in 1996 and in 2018 (fig.3)

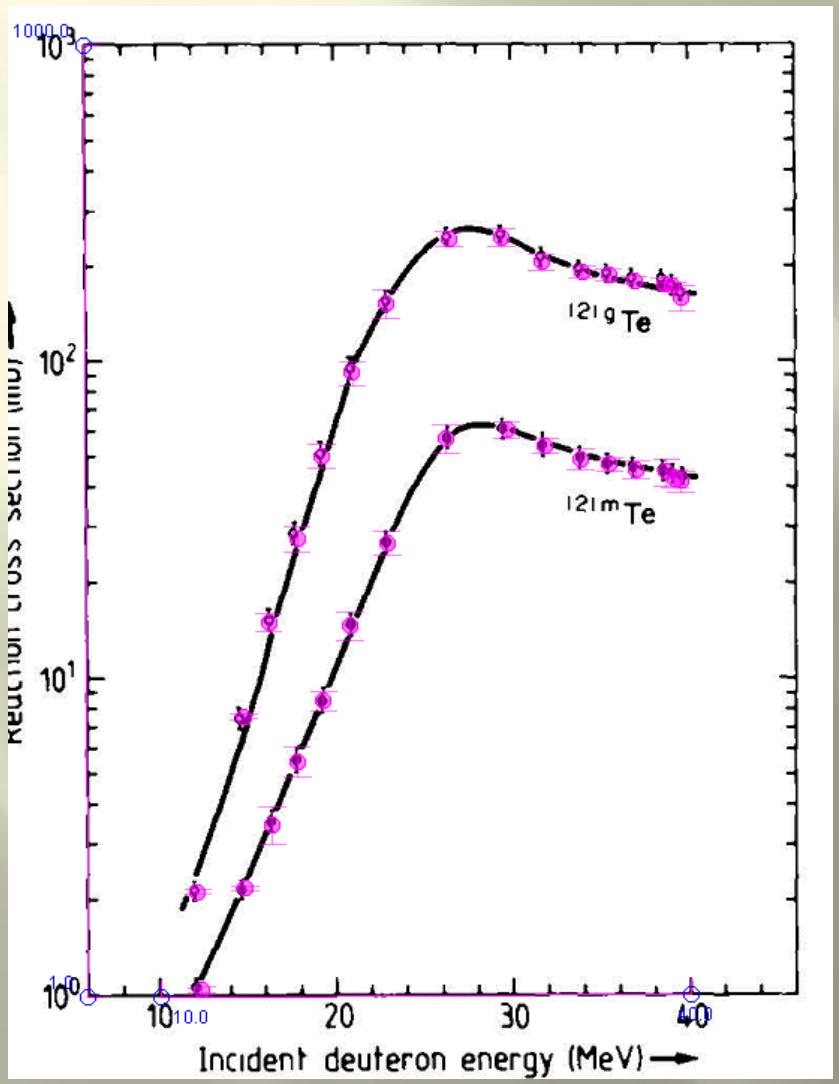

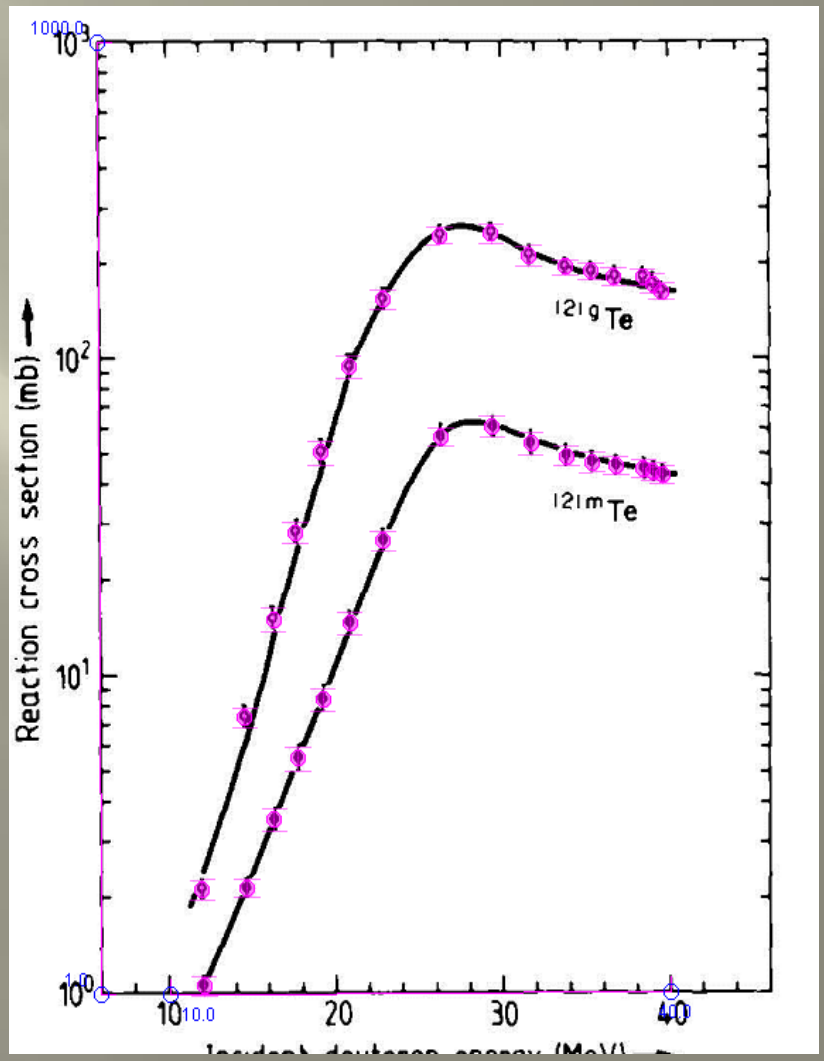

Nucl.Phys. A293(1977) 189 O1827 entry

2.B: 2.L

Nuclear Physics A293 (1977) 189–196; © *North-Holland Publishing Co., Amsterdam*

OCTUPOLE-STRENGTH CONCENTRATION OBSERVED IN α-SCATTERING ON ^{27}Al

C. MAYER-BÖRICKE, W. OELERT, A. KISS, M. ROGGE, P. TUREK and S. WIKTOR

Institut für Kernphysik der KFA Jülich, D-5170 Jülich, W. Germany

Received 1 July 1977

Abstract: Angular distributions for inelastic α-scattering on ^{27}Al were measured at E_α = 145.0 MeV. The data were analyzed for excitation energies less than 14 MeV. A strong group of levels with maximum intensity around 7.2 MeV excitation energy having a bell-shape like envelope with a FWHM of about 4 MeV was observed. The group shows strong octupole strength as deduced by comparison of the experimental results to DWBA calculations.

E NUCLEAR REACTIONS ^{27}Al(α, α'), E = 145 MeV; measured $\sigma(E, \theta)$. ^{27}Al deduced strong E3 (and E2) strength around E_x = 8.5 MeV. DWBA calculations.

1. Introduction

Mass A = 25 nuclei have predominantly prolate deformation, whereas ^{28}Si, on the other hand, has properties which can be ascribed to an oblate deformation. The nucleus ^{27}Al is in the transition region. Some controversy has arisen concerning how to describe this nucleus and its low-lying levels [1]. Weak coupling, strong coupling, and rotational-vibrational interaction approaches have been employed. Up to now, a great deal of experimental information on ^{27}Al has been available for low-lying levels and for the isoscalar giant quadrupole resonance (GQR) [2]. In this paper, we discuss the intermediate excitation-energy range between these two regions. In the case of α-scattering on ^{27}Al, a compact group of levels is selectively populated. While we restrict ourselves to the case of ^{27}Al, it should be mentioned that this seems to be a general feature of (α, α') spectra for sd shell nuclei such as the Mg isotopes [2]. While a similar selective population of the intermediate energy range is observed in the Mg isotopes, there seems to be a definite mass dependent difference. This will be a matter of further investigations.

2. Results

A typical (α, α') energy spectrum from the investigation [2] of the GQR is shown in fig. 1. The experiment was performed using the 145 MeV α-beam of JULIC (Jülich Isochronous Cyclotron). The scattered particles were detected and identified by

conventional ΔE-E techniques. The experimental details are described elsewhere [3]. The target was a 15 mg/cm^2 thick ^{27}Al foil. The energy resolution was typically 250 keV FWHM.

Only the 145 MeV α-scattering data are discussed here. However, results from experiments at several other incident energies between 106.0 and 172.5 MeV [ref. [2]] are consistent with these data. A compact group of levels was always observed at an excitation energy between 4 and 14 MeV.

To display this group more clearly, the energy spectrum of 145 MeV α-particles scattered on ^{27}Al at 7° (lab) is shown in more detail in fig. 2. Even though at excitation energies of more than 5 MeV the level density is known to be high [4], a selective population occurs in the α-scattering experiment. Furthermore, it should be stressed

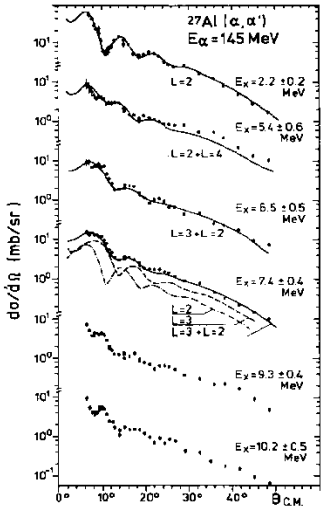

Fig. 3. Typical angular distributions of yields observed in the intermediate region. For comparison, the angular distribution for the $\frac{7}{2}^+$ level at 2.2 MeV is shown. The curves represent DWBA calculations. Only statistical errors due to counting rate are included.

Digitization in 2008 and in 2018 (fig.3)

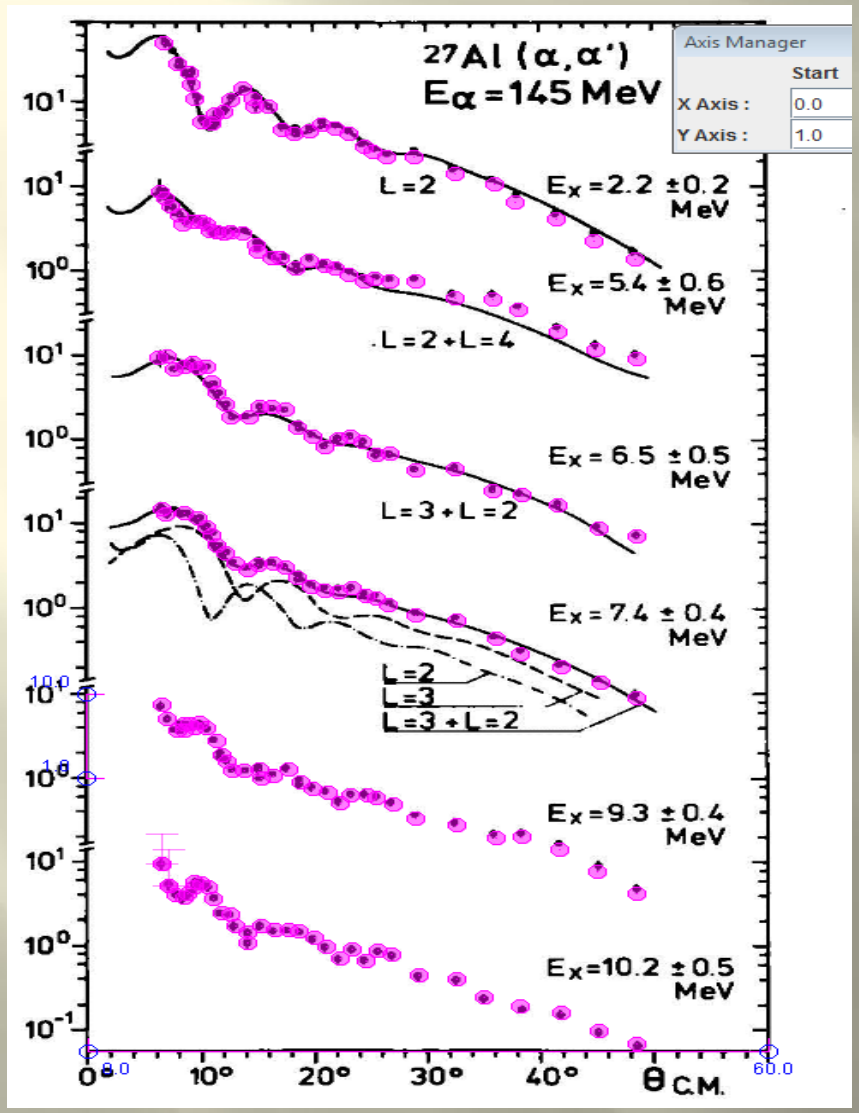

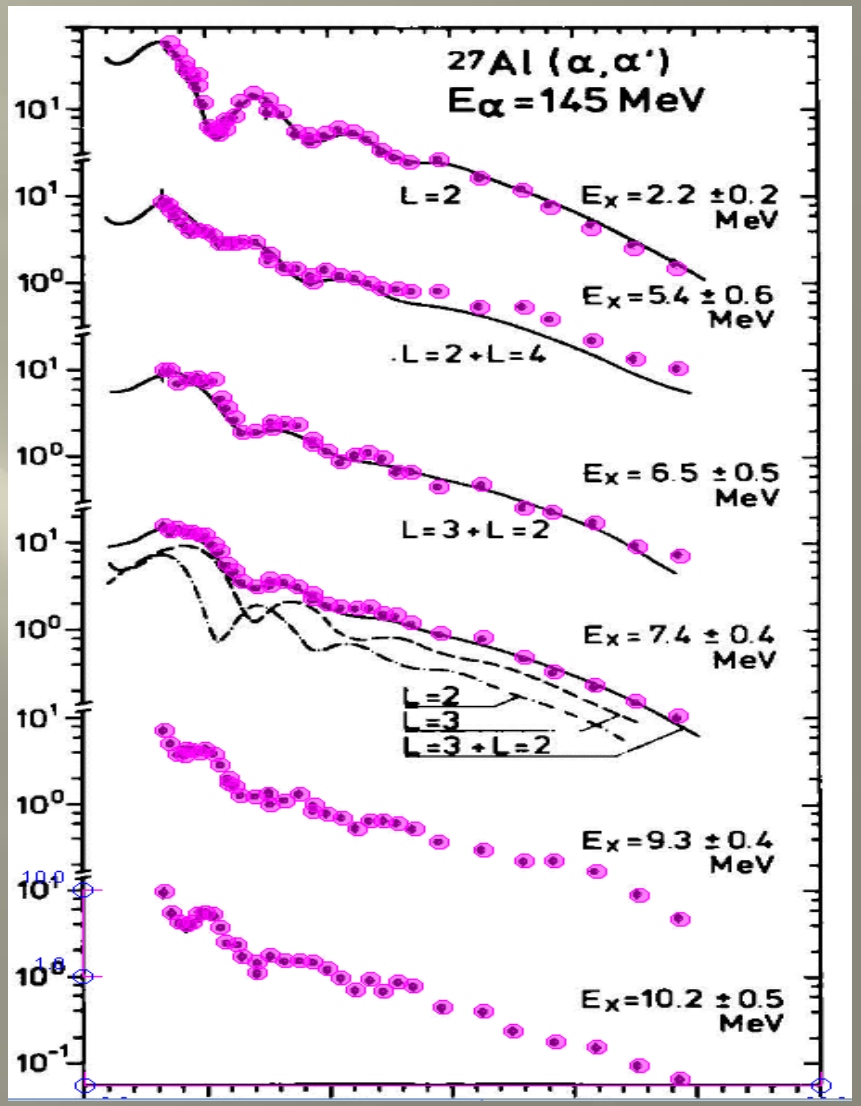

Finally,

- usually uncertainty in scale gives additionally 1-2% in old data

-not equal 90.degr. angle or really non-linear scales (more than 2%) can give different percentage of uncertainty in data

-percentage of really bad quality of figures in old publications is quite small.

- the most sensible thing in digitization is axes definition.

influence of non-linear axes on visualization using GSYS

Example(Can.J.of Phys.,52,1421,1974) (source –table data, from 10386)

CJP, 52, 1421, 74(Aug) 10386

Cross Section Measurements for the $^{103}Rh(n,n')^{103}Rh^{m}$ Reaction from[1] 0.122 to 14.74 MeV

D. C. SANTRY AND J. P. BUTLER

Chalk River Nuclear Laboratories, Atomic Energy of Canada Limited, Chalk River, Ontario

Received February 6, 1974

Cross sections for the production of $^{103}Rh^{m}$ were measured by the activation method. At energies below 5.3 MeV the neutron flux was measured with a calibrated neutron long counter, while at higher energies, measurements were made relative to the known cross section for the $^{32}S(n,p)^{32}P$ reaction. The shape of the Rh excitation curve is discussed in terms of known energy levels in ^{103}Rh. An effective cross section for a ^{235}U fission neutron spectrum calculated from the measured excitation curve is 724 ± 43 mb.

Les sections efficaces pour la production de $^{103}Rh^{m}$ ont été mesurées par la méthode d'activation. Aux énergies inférieures à 5.3 MeV, le flux de neutron a été mesuré avec un long compteur calibré, alors qu'aux énergies plus élevées on a déterminé les sections efficaces relativement à celle de la réaction $^{32}S(n,p)^{32}P$. La forme de la courbe d'excitation de Rh est discutée en termes des niveaux d'énergie connus pour ^{103}Rh. La valeur effective de la section efficace pour le spectre des neutrons de fission de ^{235}U calculée à partir de la courbe d'excitation mesurée est 724 ± 43 mb.

[Traduit par le journal]

Can. J. Phys., 52, 1421 (1974)

Introduction

Because of its low effective threshold energy (40 keV) rhodium is considered an important fast neutron flux monitor, especially for nuclear reactors. The isomeric state at 40 keV in ^{103}Rh decays with a half-life of 56 min and can be produced by neutron inelastic scattering by either direct excitation or more probably following excitation to higher levels which de-excite immediately to the isomeric state. The 40 keV transition is highly internally converted so that the observed radiation consists almost entirely of *K* X rays of ~20 keV energy.

As a continuation of our previous studies to provide a set of precise fast-neutron excitation curves for threshold detectors, this paper describes measurements of the $^{103}Rh^{m}$ production cross section from threshold energies to 14.7 MeV. A detailed description is given of measured corrections which were required for cross section determinations.

Experimental Work

In a previous publication (Santry and Butler 1972) a complete description was given of the equipment and techniques which are used in our cross section measurements. Therefore, only a brief outline of the experimental arrangement will be given here with emphasis placed on those newer features which applied specifically to Rh activation and activity measurements.

Irradiations

Listed in Table 1 are nuclear reactions used to produce monoenergetic neutrons.

Lithium targets were prepared by vacuum sublimation of LiF onto gold backing foils. Measurements of the neutron yield (0°) as a function of proton energy showed the well known two maxima; one a threshold at 1.881 MeV and the other a resonance at 2.27 MeV. The thickness of each target was determined by weighing and by measuring the energy shift of the resonance, *i.e.* the difference between the proton energy at threshold and the proton energy corresponding to the resonance. Agreement between the two methods was 5%. Typical target thicknesses were 500 μg/cm² which corresponded to an energy loss of ~60 keV for 2 MeV protons.

By cooling the irradiation cell with a jet of air, the LiF targets could be operated with beam currents up to 20 μA over an 8 mm² area for several hours without any appreciable decrease in neutron yield.

Targets of Ti–T and D_2 gas were also used and these were identical to those described previously (Santry and Butler 1972).

Disks of Rh metal 4.76 mm in diameter and

[1]AECL 4819.

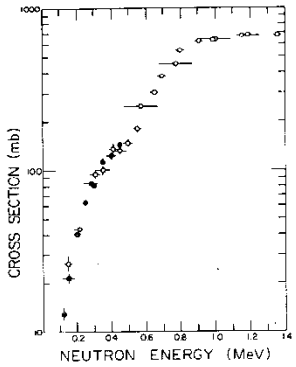

FIG. 5. Measured $^{103}Rh(n,n')^{103}Rh^{m}$ cross section. Neutron source ● ($^{7}Li + p$), ○ ($T + p$).

cross section at 13.58 MeV. Neutrons produced at this energy with the (D + D) reaction required a large breakup correction while neutrons produced with the (D + T) reaction required no correction.

Results and Discussion

Cross section values for Rh based on neutron flux measurements made with a calibrated neutron long counter are given in Table 2. At neutron energies >4.8 MeV, Rh cross sections were measured relative to the $^{32}S(n,p)$ reaction and the results are listed in Table 3. Continuity in the shape of the cross section curve, as shown in Fig. 5, was obtained in the low energy region where neutrons were produced with the (p + Li) and (p + T) reactions.

In the energy region 4.8 to 5.1 MeV, 10 irradiations were performed and cross sections were calculated relative to both the neutron long counter and the sulfur monitors. The average values agreed to within 2% which was well within the accuracy of the two methods. It should be emphasized that fluxes measured with the long counter were in no way normalized to the $^{32}S(n,p)$ measurements.

Good agreement was obtained in other energy regions where neutrons were produced from different reactions, *i.e.* ~5 and 13.6 MeV. The complete excitation curve is shown in Fig. 6.

Each cross section is the average of at least two determinations. Errors in the measurements were described in detail previously (Santry and Butler 1972) and include an uncertainty in counting efficiency, sample-to-monitor geometry factor, corrections due to the presence of extraneous neutrons, and also, statistical counting errors. In general, the errors in cross section values are about 4 to 6% except near the reaction threshold energy. Neutron energies listed are average values with 68% of the neutrons having energies within the range quoted. Errors in the neutron flux measurements are 3 to 4% for the long counter and 3% for the $^{32}S(n,p)$ measurements.

A comparison of our measurements with those of other investigators is limited to three sets of data. Some relative cross sections were measured by Garvey (1963) and these results when normalized to our data at 3.3 MeV, reproduce the shape of our measured excitation curve from 0.2 to 5 MeV. From 5 to 7.8 MeV, the normalized values of Garvey are lower than our measured values. No experimental details were given concerning the measurements by Garvey nor were any errors quoted for either neutron energies or the cross section values. Nagel and Aten (1966) measured a value of 508 ± 50 mb at 14.2 MeV. Our value at this energy is 297 ± 13 mb. Kimura *et al.* (1969) measured cross section values at energies from 0.180 to 4.6 MeV. Their results were about 30% lower than ours. Kimura gives no indication that corrections were applied to their data for the various effects described in our papers. We assume that such corrections were not measured. In addition, the actual efficiency factor for X ray counting their Rh samples was not given; consequently, it is not possible to evaluate their radioactivity measurements.

Cross Section Value for a Fission Neutron Spectrum

The effective cross section $\bar{\sigma}$ for Rh in a ^{235}U fission neutron spectrum was calculated from

$$\bar{\sigma} = \int_0^\infty N(E)\sigma \, dE$$

Difference in GSYS presentation

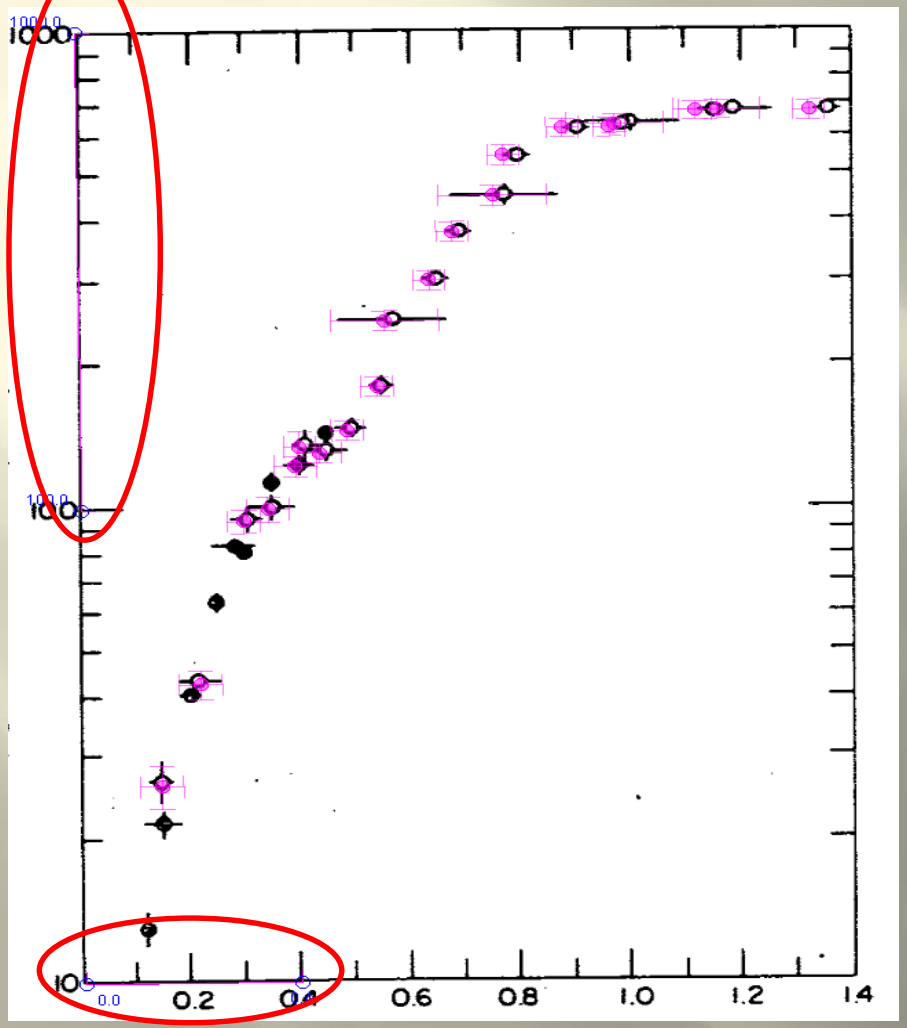

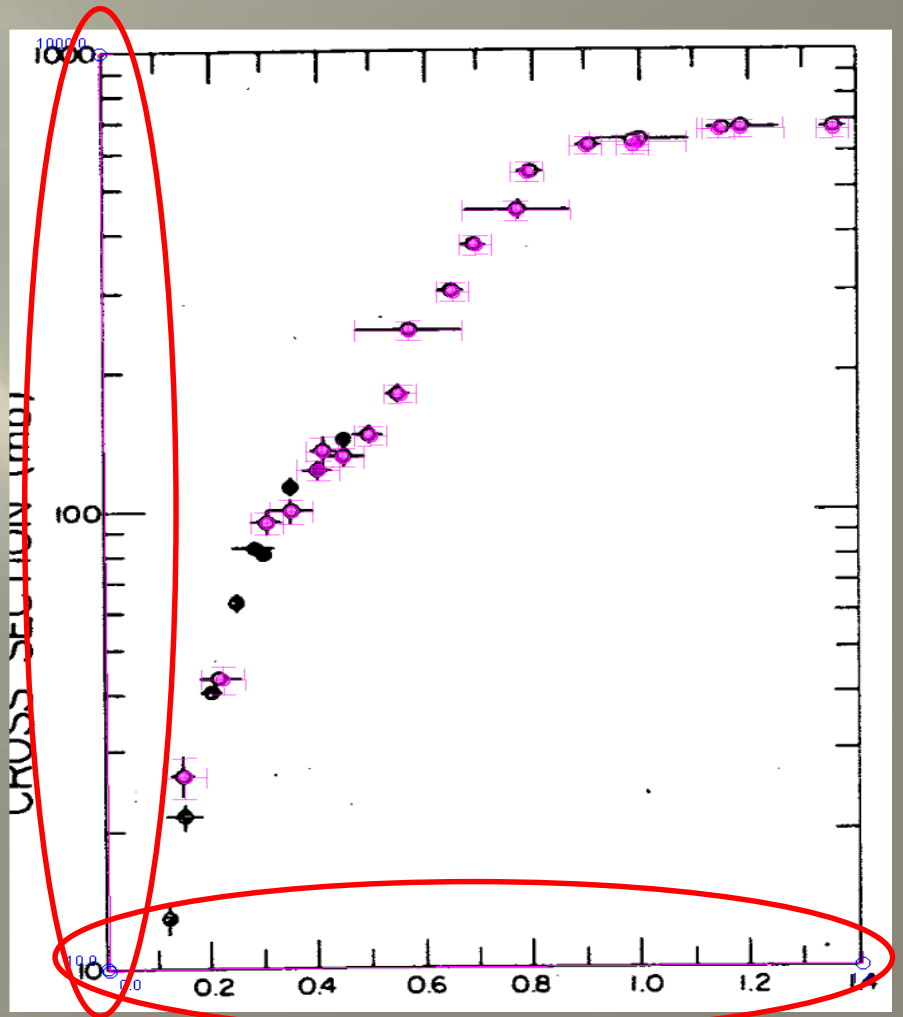

Example from Appl.Rad.&Isot.,26,71,1975(fig.4(b)) 20866

International Journal of Applied Radiation and Isotopes, 1975, Vol. 26, pp. 71–76. Pergamon Press. Printed in Northern Ireland

The Use of a Small Accelerator to Study the Gamma Rays Associated with the Inelastic Scattering of 14-MeV Neutrons in ^{28}Si, ^{32}S and ^{48}Ti

K. A. CONNELL and A. J. COX
Physics Department, University of Aston in Birmingham, Birmingham, England

(*Received* 19 *April* 1974)

The γ-rays associated with the inelastic scattering of 14-MeV neutrons in ^{28}Si, ^{32}S and ^{48}Ti are investigated. In each case the differential cross section in the range of 0–90° are measured with angular resolution of ±4°. The neutrons are produced using the $^2D(T, n)^4\alpha$ reaction. A time-of-flight technique using the α particle associated with production of the neutron to give a zero time signal is used to reduce background interference.

AT PRESENT there is a lack of data on γ-rays produced in fast neutron reactions and little information concerning the reaction mechanisms. Most of the work to date has been done with neutrons whose energies are less than 7 MeV. What work has been done in the 14–15 MeV region has concentrated on the measurement of differential γ-ray cross sections and usually measurements are made at 90° only, with angular resolutions in the region of ±20°. Measurement of the angular distributions of emitted γ-rays can give much needed data for the shielding of fast reactors and other intense neutron flux devices. In addition they are interesting theoretically as they provide a test of the reaction mechanism.

The present work investigated the angular distributions of the γ-rays associated with the inelastic scattering of 14-MeV neutrons produced by the $T(D, n)\alpha$ reaction. Time-of-flight techniques were used both to differentiate between γ-rays and neutrons and to reduce background interference. The angular resolution was ±4°. The elements investigated were ^{28}Si, ^{32}S, ^{48}Ti, each of which was selected as each has ground state spin of 0^+ and a first excited state spin of 2^+ and have been relatively little investigated at 14 MeV. In each case where more than a single previous measurement had been made there were discrepancies in the reported results.

The experimental arrangement is shown in Fig. 1. The 150 keV deuteron beam from a SAMES type J accelerator was incident on a tritiated titanium target. The α-particle produced a zero time signal. The neutrons were inelastically scattered from the scattering sample and the resultant γ-rays detected by the moveable NaI(Tl) detector 1·39 m. from the scattering sample. The γ-ray detector and its shield are shown in Fig. 2. A 76·2 mm × 76·2 mm NaI(Tl) crystal was mounted, via a converging perspex light pipe (angle of convergence 9°), onto a 2-in. 56 AVP photo-multiplier tube fitted with a μ-metal shield. The NaI was shielded from randomly scattered γ-rays and neutrons by the shield and from the neutron source by means of the iron shadow bar. NaI(Tl) was used as the detector, because of its greater efficiency and smaller neutron response compared to a Ge(Li) detector in the present experimental situation. It is also less susceptible to damage caused by continued exposure to fast neutrons.

The emitted α-particles were detected by a NE 102a plastic scintillator sheet ($\frac{1}{8}$ mm thick) manufactured by Nuclear Enterprises Limited mounted on a 56 AVP photo-multiplier tube

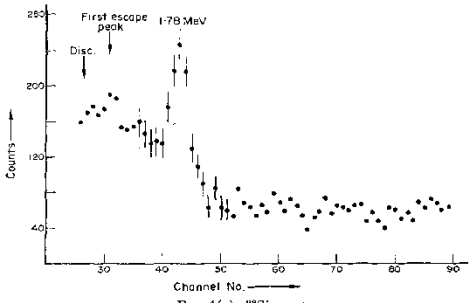

FIG. 4(a). ^{28}Si spectrum.

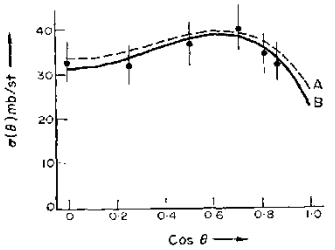

FIG. 4(b). 1·78-MeV γ-ray angular distribution: (a) MARTIN and STEWART;[5] (b) Present work.

Table 1 compares the present 90° differential cross-section measurement with other published work.[5–6] It also gives the various experimental techniques used and the angular resolutions achieved by the authors quoted.

The angular distribution was fitted by the least squares method to an even order Legendre polynomial series. The equation fitting this curve is

$$\sigma(\theta) = (31{\cdot}5 \pm 1{\cdot}6) + (38{\cdot}4 \pm 11{\cdot}7)\cos^2\theta - (48{\cdot}5 \pm 13{\cdot}4)\cos^4\theta.$$

The integrated cross-section has a value of 434 ± 63 mb which is mid-way between Martin Stewart's results and those of BENETSKII[7] with values of 471 ± 70 mb and 370 ± 60 mb respectively.

Results for sulphur

The same experimental procedure and analysis as above was used here. The sample consisted of a fused block of sulphur 100 × 120 × 27·7 mm with a density of 1980 ± 10 kg/m^3. Spectra were accumulated at 90°, 70°, 60°, 40° and 25° and a typical spectrum is shown in Fig. 5(a). Three peaks are clearly visible at 2·24, 1·7 and 1·2 MeV, respectively. The only non-negligible mechanism for producing these is the $^{32}S(n, n')^{32}S$ reaction exciting both the first excited state of ^{32}S at 2·24 MeV and higher excited states which populate the 2·24 MeV level with subsequent γ-ray de-excitation; the peaks at 1·7 and 1·2 MeV correspond to the first and second escape peaks. The angular distribution is shown in Fig. 5(b) together with the fitted curve.

$$\sigma(\theta) = (18{\cdot}4 \pm 0{\cdot}9) + (58{\cdot}2 \pm 6{\cdot}6)\cos^2\theta - (46{\cdot}2 \pm 7{\cdot}8)\cos^4\theta.$$

The shape of our curve is less anisotropic than that of Martin and Stewart. The integrated cross-section was found to be 318 ± 36 mb. Our results are compared to other author's results in Table 2. It will be noted that the

Difference in GSYS presentation

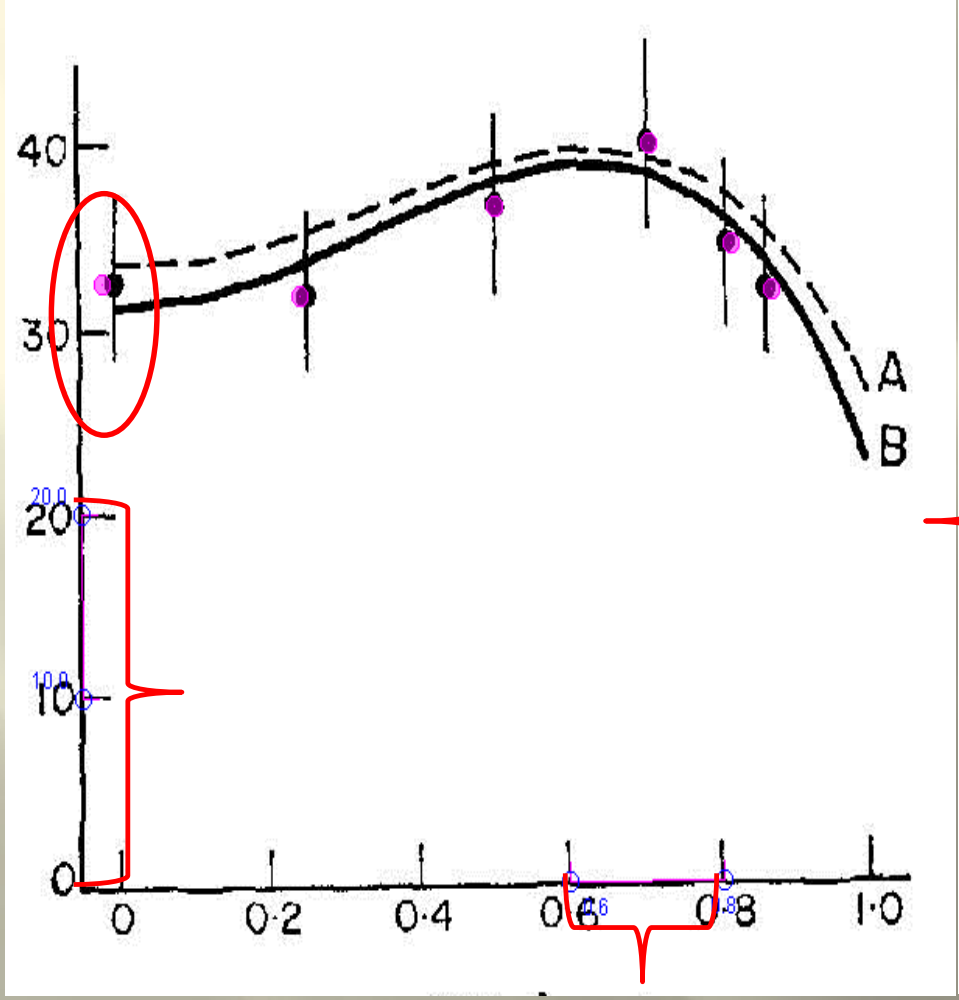

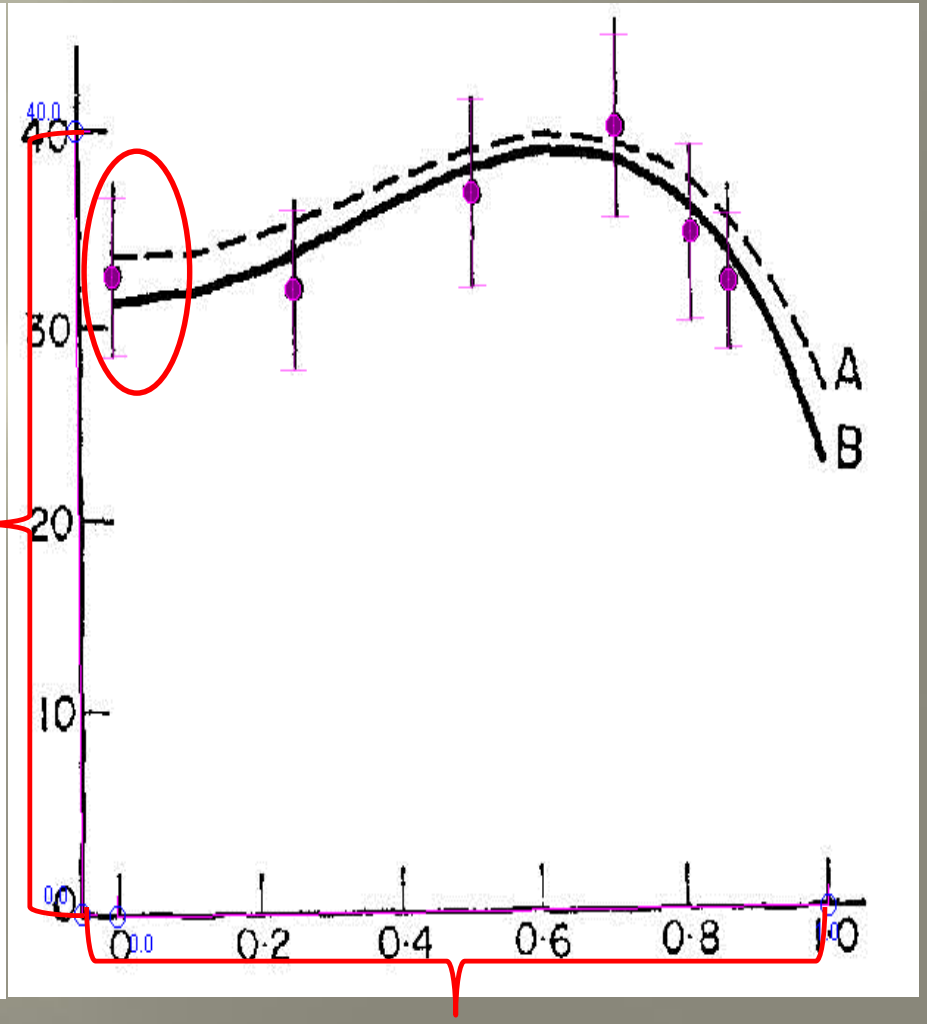

CONCLUSIONS
(only for old publications)

Better to:

1. not forget to check digitized data revising old Entries, especially, if digitization was made before 1998 for old publications when set of ordinates for different sets of points are given on one figure;
2. add abscissa/ordinate axes or direction line in every case (if it is possible);
3. define scales for full set of points in both cases (digitization or visualization).
4. be careful in using GSYS for visualization of old data.

Thank you!